Neurotransmitter MIPs for the Potential Use in Amperometric Sensors

A Master's Thesis by

Axel Rüter

Main Supervisor
Lei Ye

Examinator
Per-Olof Larsson

LUND
UNIVERSITY

Department of Pure and Applied Biochemistry
Faculty of Engineering

In Cooperation With
Department of Biomedical Science
Malmö University

Abstract

Molecular imprinting technology is a field where polymer technology is utilised to synthesise high affinity particles, much like antibodies. This project has dealt with the imprinting of the neurotransmitter molecules serotonin and histamine. Serotonin polymers were synthesised using methacrylic acid and acrylamide as functional monomers relying on hydrogen bonding for the imprinting effect. None of the produced batches showed any sign of imprinting. Instead histamine polymers were successfully synthesised showing specific binding with the average binding affinity $K_d = 0.61$ mM and the approximate number of binding sites $N = 50\ \mu\text{mol}\,\text{g}^{-1}$. In a cross-reference rebinding test with serotonin the histamine particles showed higher binding but less specificity. The reason for this is presumably the hydrophobic nature of both serotonin and the cross-linking monomer in the polymer. Novel tries were made of immobilisation of imprinted particles on to a gold electrode by physical adsorption and by electrochemical cleaning. This would give an idea of how to apply molecularly imprinted particles in sensing devices.

Acknowledgements

I would like to start by sending my thanks to my supervisors, Lei Ye, Börje Sellergren and Sergey Shleev for making it possible to work on this project and for the valuable input used to bring the project forward.

A special thanks to Sudhirkumar Shinde, Elena Gonzáles Arribas, Yeung Sing Yee, Celina Wierzbicka, Mark Galat and Dmitry Pankratov for helping and supervising my experimental work. Thank you also to the rest of the employees, guest researchers and students at the Department of Biomedical Science at Malmö University that I have met during my stay. It has been a good time both in and out of the lab.

Finally I would like to thank my family and friends that have supported me during my work.

List of Figures

List of Abbreviations

ABDV	2,2'-azobis(2,4-dimethyl valeronitrile)
AFM	atomic force microscopy
AIBN	azobisisobutyronitrile
AM	acrylamide
AuNP	gold nanoparticle
$C_3H_5ClO_2$	ethylchloroformate
CE	counter electrode
$CHCl_3$	chloroform
CL	cross-linker
CPDB	4-cyanopentanoic acid dithiobenzoate
DLS	dynamic light scattering
DMF	dimethylformamide
DMSO	dimethyl sulfoxide
EGDMA	ethylene glycol dimethacrylate
FRP	free radical polymerisation
HPLC	high-performance liquid chromatography
M	functional monomer
MAA	methacrylic acid
MAam	methacrylamide
MeCN	acetonitrile

NMR	nuclear magnetic resonance
PBS	phosphate buffered saline
RAFT	reversible addition-fragmentation chain transfer
RE	reference electrode
redox	reduction-oxidation
RP-HPLC	reversed phase HPLC
SEM	scanning electron microscopy
SiNP	silica nanoparticles
SPR	surface plasmon resonance
T	template
TEA	triethylamine
TEM	transmission electron microscopy
THF	tetrahydrofuran
UV-Vis	ultraviolet-visible spectrophotometry
WE	working electrode

Contents

1

Introduction

When it comes to molecular recognition, nothing beats nature. The interaction between an antibody and an antigen might not be more than some chemical bonds, but their exact placement and numbers help the body distinguish between friend and foe. This high specificity of the antibodies is commonly used in medical applications of today [1]. Even though this technology has brought a lot of progress to the field of medical diagnostics, it still suffers from some practical limitations. Antibodies taken from their natural environment are not as stable which makes them hard to implement in for example industrial fabrication of medical devices. They are also expensive to produce and use.

Molecular imprinting technology is field with the goal of producing synthetic materials with high specific affinity for a molecule, much like an antibody. The technology can be explained as a type of chemical molding, by which cavities are created in a polymer matrix that fit a specific molecule. The similarity to antibodies, but with a cheaper production and a greater stability, gives hope that once refined, molecularly imprinted polymers (MIPs) will be able to revolutionize areas such as the sensor and the separation industries.

1.1 Thesis Background

Serotonin is a molecule of great interest. It is a neurotransmitter which can be found both in the gastrointestinal tract and in the central nervous system of the human body and it is in many ways involved in processes that regulate hunger and mood [2, 3]. In many of the medications for treatment of depression, anxiety and eating disorders, active substances block the re-uptake of serotonin to the presynaptic neuron causing a higher extracellular concentration. Measurement methods today can for example involve immunoadsorb-

ing or chromatography methods [4], time and money consuming measurements. An easier way of measuring serotonin levels in either serum or other bodily fluids would be beneficial.

Successful imprinting of serotonin has already been done [5, 6], but only fairly recent, and the fact that serotonin is a very unstable molecule if not handled correctly makes the procedure a bit difficult. The idea of incorporating these MIPs in an amperometric sensor is however new, even if sensing systems in other formations have been approached [7].

1.2 Objective

The objective of the thesis was to take one part of MIP technology which is fairly known: the imprinting of small biomolecules, and try to conceptualise this process towards a future product. The product idea: an amperometric sensor for the neurotransmitter serotonin in bodily fluids. At a first stage the concepts of molecular imprinting was learnt and practised before the sensor concept could be approached. This would start out as macro scale tries, but if there was time the system should also have been scaled down. A smaller size would reduce both the amount of material used in the construction, but also the amount of analyte, two important points in working towards products.

The idea for the thesis arose from the cooperation between two research groups at Malmö University. The organic chemistry with MIP synthesis and analysis is based on the work of Börje Sellergren's group. Their current work is focused on imprinting of larger peptide structures, but also on the synthesis of small MIP core shell composites and the imprinting of neurotransmitters [6]. Through the faculty of Health and Society there is a connection to Sergey Shleev and his group working on electrochemistry, where they are developing a tear liquid micro sensor for detection of specific bioanalytes [8].

1.3 Problem Formulation

This thesis can loosely be divided into three parts. For the first part molecular imprinting will be in focus. Background questions such as how it works on a molecular level, what forces are behind the chemistry of imprinting, should be possible to answer. These very theoretical questions should also be extended to include experimental analysis; how are MIPs characterised and what properties of such a system can be quantified? Also to answer is

how properties of MIPs are altered, what parameters during synthesis affects the outcome?

The second step handles the incorporation of the MIPs on the sensing element. How can the MIPs efficiently be immobilised on to the sensor surface? What measures can be taken to ease the process and what properties does one need to keep in mind for such a system to show appropriate response? What geometry should the MIPs have, and how should they behave chemically? Will it be possible to covalently bind the particles or will physical adsorption be enough?

Finally there is the electrochemical part that should answer questions about how a sensor would be set up and the theory behind the transformation from a biological molecule to a detectable electrical signal.

1.4 Workflow and Methods

The work of the project was of both experimental and theoretical character. It started out with electrochemical and other chemical analysis of prepolymerised core-shell serotonin MIP particles using mainly cyclic voltammetry and spectroscopy methods. After that the process of working with pure MIP synthesis and analysis took over. Serotonin was at first the main target but the project also got expanded to include histamine.

As mentioned, the first part consisted of electrochemistry and in specific cyclic voltammetry. For the other chemical analysis of the presynthesised particles analytical MIP characterisation techniques were used, such as chromatographic methods, spectroscopic methods and nuclear magnetic resonance. The same analytical methods was also utilised for analytical characterisation of the MIPs synthesised by myself. The synthesis of bulk serotonin MIPs was followed by a lot of problems and was therefore combined with a great deal of troubleshooting. A successful imprinting was however achieved with the histamine system where some more theory in mathematical curve fittings and calculation of important MIP parameters was practised.

The layout and contents of this report has its main focus around molecular imprinting theory, as this was the main focus of the project.

2

Molecular Imprinting

2.1 Background

The whole concept of molecular imprinting is often explained by the lock and key analogy, where the key is a small molecule of interest fitting into the created lock construction. One lock type holds only one type of key and high specificity can be reached. This is often compared to how antibodies function. The design and creation of the lock construction relies on organic chemistry. By synthesising a cross-linked polymer network around the template molecule, a stable and cheap way to produce molecularly imprinted polymers is achieved.

There are different approaches to molecular imprinting, which are generally divided by the interaction type that occurs between the template and the polymer [9]. Those can be either covalent, semi-covalent, non-covalent or coordination with metal ions. Each of which has its advantage and disadvantage. The covalent approach creates strong covalent bonds between the template and the monomers during the synthesis stage. This method was developed mainly by Günther Wulff with colleagues and was the first method used for molecular imprinting. The binding sites created in this process show a very stable morphology corresponding to the imprinted template, meaning that the binding sites throughout the matrix are relatively uniform and should lead to sites with higher affinity [10]. The need for the covalent bond to be fully reversible and that the molecules for this are not that abundant are some of the drawbacks of this approach.

The more commonly used non-covalent approach was mainly developed by Klaus Mosbach and colleagues. The method relies on non-covalent bonds such as hydrogen bonds, hydrogen bonded ion pairs, van der Waals interactions and hydrophobic interactions. These types of bonds are by nature reversible, on the other hand also approximately $1-3$ orders of magnitude

weaker than covalent interactions. By combination of such bonds stronger binding can be reached [9]. When working with non-covalent interactions, the MIPs generally have lower binding capacities due to a large amount of unwanted non-specific binding. This is due to competing interactions between all reactants during the synthesis, for example hydrogen bonding between template and solvent.

In this thesis the non-covalent approach is used and discussed.

2.2 MIP Constituents

The process of molecular imprinting is schematically shown in Figure 2.1 and consists of the following constituents: the template molecule (T), which is the molecule or other type of structure that one wants to bind, the functional monomer (M) which is the building block of the polymer matrix, the cross-linker (CL) that chemically glues the building blocks together to create a both chemically and physically stable matrix, and finally the porogen or the solvent in which the imprinting process is carried out. All of these play a big role in how the final polymer will behave. Other factors that have an impact are the choice of polymerisation technique, method of initiation, temperature and pressure to mention some.

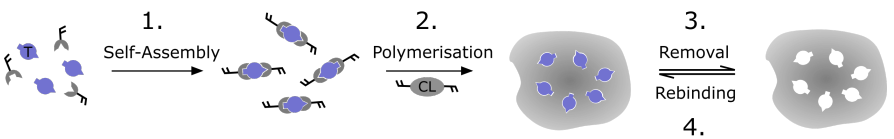

Figure 2.1: *A schematic figure showing the main steps in molecular imprinting. A mixture of the template (T) and functional monomers are dissolved in the porogen and let to self-assembly (1). The template-monomer complexes are polymerised (2) in the presence of a cross-linker (CL) to form a stable polymer network. The template has to be removed (3) before further testing can be performed including the rebinding of the template to the polymer (4).*

A reference polymer should be synthesised and further handled in exactly the same manner, except for the omission of the template molecule. Such a nonimprinted material is often referred to as nonimprinted polymer (NIP).

2.2.1 The Template

The target of the imprinting process can range from low molecular weight compounds such as steroids, pharmaceuticals or neurotransmitters, to larger ones including oligopeptides or even whole proteins. A suitable template should fulfil a number of criteria: it should have the ability to produce specific interactions with the functional monomer(s) through functional groups or other properties, it should withstand the sometimes rough environment of the polymerisation process, it should be soluble under the used conditions, and it should preferably be cheap and abundant. Analytes not fulfilling these criteria could be switched for a so called template analogue, which is either a derivative of the original template or a compound with similar structure.

2.2.2 Monomer Selection

The key of molecular imprinting lies in the specific interactions between template and functional monomer. Therefore the choice of functional monomer(s) for the process is very important. These building blocks must have properties that complement the functionality of the template to create as strong interactions as possible. An acidic monomer is able to produce fairly strong electrostatic interactions with a basic template and vice versa.

The most common example of a functional monomer is MAA [9], its structure shown in Figure 2.2a. The carboxylic acid group has the possibility to form a large variety of bonds. MAA is known to be both a good hydrogen bond donor through its hydroxyl group but also a good acceptor due to the electronegative oxygen in the carbonyl group. It is also possible for a basic group to attract the acidic proton and thus create an electrostatic interaction.

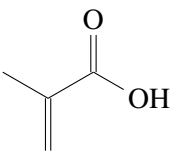

(a) *Methacrylic acid.*

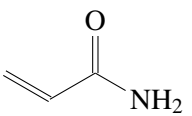

(b) *Acrylamide.*

Figure 2.2: *Metachrylic acid is one of the most used functional monomers in molecular imprinting, with properties that favour hydrogen bonding. Its acid can also take part in strong ionic interactions with bases. Acrylamide is a neutral monomer that can be used either as a hydrogen bond acceptor or for neutralisation of the final polymer.*

It is also possible to use basic or uncharged monomers. Acrylamide, shown in Figure 2.2b, is sometimes used as a functional monomer. Its amide oxygen has the possibility to act as a hydrogen bond acceptor. Both acrylamide and other neutral monomers, such as methacrylamide and styrene, can however also be used specifically for its uncharged properties, acting as a spacer between the non-neutral monomers [5]. By increasing the amount of neutral monomers, the final polymer itself will be less charged and therefore show less non-specific binding.

During the imprinting process a cross-linking monomer is used to produce a highly cross-linked polymer and stable binding sites. The ratio of CL to functional monomer(s) is of high importance, a greater amount of CL monomer added to the mixture will produce a more brittle polymer. A commonly used CL is EGDMA, shown in Figure 2.3.

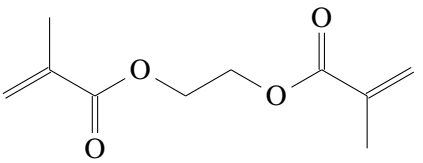

Figure 2.3: *Ethylene glycol dimethacrylate is commonly used CL monomer. It acts as a glue, stabilising the finished polymer and its binding sites.*

2.2.3 The Porogen

The first thing to consider regarding the porogen is the solubility of all the different components to be used during the synthesis. Secondly the porogen should not interfere with the template-monomer complex. In an imprinting relying on mainly hydrogen bonds for example, a protic solvent such as methanol or water should be avoided. Instead acetonitrile (MeCN) or dimethyl sulfoxide (DMSO) could be considered. The polarity of the porogen also plays an important role. In a case where the imprinting relies on electrostatic and van der Waal forces a very polar porogen can interfere with these. Commonly used non-polar porogens are chloroform ($CHCl_3$) or toluene.

One might think that the best porogen then always is non-polar and aprotic, but that is far from a rule. Synthesised MIPs tend to exhibit best properties in the solvent which the polymer itself was prepared [11]. A porogen should therefore also be chosen with the final application in mind.

2.2.4 Polymerisation Methods

MIPs are ususally synthesised through free radical polymerisation (FRP) [12, 13]. In this method free radicals are generated and are let to react with unsaturated carbon-carbon bonds to create growing chains [14]. Free radical polymerisation runs through three main steps: initiation, propagation and termination. During the initiation the radicals are created by thermolysis or photolysis of the initiator. In the propagation stage the polymer chains are growing by continuously reacting with unsaturated carbon-carbon bonds. The reaction is finally terminated by either combination or disproportionation.

Conventional free radical polymerisation is usually more tolerant on functional groups in comparison to for example ionic polymerisation [13], it is also very simple to prepare and does not require any sophisticated equipment. A very heterogeneous network structure is produced due to the inability to control the properties such as termination and chain propagation. This has led to the introduction of controlled radical polymerisation techniques in MIP technologies.

RAFT Polymerisation

One type of controlled radical polymerisation method is reversibel addition-fragmentation chain transfer (RAFT) polymerisation. This method shows the same positive properties as FRPs but in combination with a higher control for the end polymer. To a conventional FRP a RAFT agent or a chain transfer agent is introduced. After initiation the propagating species are trapped in a dormant state hindering termination and an equilibrium is formed between dormant and active species with the same probability of reinitiation. The final polymer has a homogeneous structure and low polydispersity which has made this method a promising tool for the synthesis of MIPs [15].

2.2.5 Template Removal

After the polymerisation, template removal from the binding sites is the necessary final step before the MIP can be analysed. The goal of reaching a full removal of the template in combination with an intact polymer structure makes this step a hard task [16]. A common washing method relies on the template extraction by solvent. This can be done in a continuous manner with Soxhlet extraction or in a non-continuous manner by simply immersing the MIPs in the washing solvent and repeatedly changing it.

When choosing the washing method one should as always consider the

consequences. Some techniques are time consuming and use a large amount of solvent, wheras some might induce a lot of material loss. The correct choice of solvent is also an important one. In a system based on acidic monomers and basic templates, an acid should be present that could reprotonate the carboxylate groups in the acid, facilitating the release of the template. Finally it is important to monitor the washing solution, this way the amount of template removed can be quantitatively determined.

2.3 MIP Formats

A common way to produce MIP is by the means of bulk polymerisation. Imprinted monoliths are synthesised and then crushed to finer particles. This method does not only produce a huge amount of material which is unused, but it is also time consuming and some times the mechanical milling leads to degradation of the specific binding sites. By instead synthesising MIP nanoparticles it is possible to reduce the amount of starting material needed, and at the same time increase the effective capacity [13]. A larger number of high affinity sites are simply more accessible when diffusion distances are shorter.

Synthesis of MIP nanoparticles can be performed using a wide variety of polymerisation methods where one way is to use a non-organic material as a starting point. Silica nanoparticles have good properties and are today widely used as core-particles for MIP composite materials. By using surface initiated RAFT polymerisation on silica particles, a core-shell structure can be synthesised. These structures with non-organic materials coated by a nanometer thick layer of imprinted polymer have interesting properties. It is a way to combine the signal transducer within the MIP material in for example binding assays and chemical sensing devices.

2.4 MIP Characterisation Techniques

There are many ways to characterise MIPs but these are mainly divided into physical and analytical characterisation. Physical properties of interest are usually size distribution, dispersity in solution, geometry et cetera. The analytical characterisation on the other hand is performed to determine if the MIP-particles function. Is there a higher binding capacity for the targeted molecule in comparison to nonimprinted material and what are the specific binding properties?

2.4.1 Analytical Characterisation

MIPs are usually analytically characterised by graphically showing the bound analyte concentration (C_b) versus the free analyte concentration (C_f). These values can be calculated from so called rebinding tests, where a simpler versions is called equilibrium rebinding or batch rebinding. For this, a known amount of MIP is subjected to a solution containing a known template concentration (C_0), for a certain amount of time. The template will, due to diffusion and mechanical stirring or shaking, bind to the sites in the polymer and after a while all accessible binding sites are full and saturation is reached. The solution will then be separated from the MIPs and analysed to determine the concentration of template still present (C_f). Template which is not free in the solvent is either bound to a binding site or non-specifically to the polymer, no discrimination is made in this step and this total concentration is the bound analyte concentration (C_b). From a standard calibration curve with the slope k and the value m at $x = 0$ Equations 2.1 and 2.2 are used to calculate the concentrations. F represents the measured value of the supernatant, usually obtained from UV-Vis absorption spectroscopy or fluorescence spectroscopy measurements, either by themselves or in combination with high performance liquid chromatography (HPLC), v is the volume of the added solution and m is the mass of polymer in the sample.

$$C_f = \frac{F - m}{k} \tag{2.1}$$

$$C_b = \frac{V}{m}(C_0 - C_f) \tag{2.2}$$

HPLC is a common separation technique used in analytical chemistry. The method analyses the molecular components of a sample by pumping it through a column with an adsorbing solid phase, the liquid carrying the analyte through the column is called the liquid phase. The components interact differently with the solid phase and will therefore take different times to run through the column. This leads to separation of the components that can be further analysed by previously mentioned spectroscopy methods. In MIP technology reversed phase HPLC (RP-HPLC) is often used to measure the functionality of the synthesised polymer by analysing the supernatant after an equilibrium rebinding test. Reversed phase HPLC uses a hydrophobic solid phase and a polar liquid phase. Another way of using chromatography in analytical characterisation is to use the MIP as the stationary phase.

2.4.2 Binding Isotherms

The plot of C_b versus C_f is the so called binding isotherm and are always measured for both the MIP and the NIP particles. For further analysis of the particles and for calculation of binding properties this data is fitted to different binding models; the simplest, homogeneous models, assume that all the binding sites in the MIP are equal, whereas heterogeneous models regard the fact that some sites have a higher affinity to the analyte than others [9]. MIPs usually show a more linear region for low C_0 whereas a saturation concentration is usually reached for higher values of C_0. What model to use depends on in what region the analysis takes place. For linear region analysis Freundlich isotherms could be used, and for the saturation region Langmuir isotherms are more valid. The models can be combined for the whole interval but these fittings require sophisticated software for the calculations. The binding properties that you can calculate with the models are usually the binding constant K and the number of binding sites N or maximum amount of analyte that can be bound to the MIP.

2.4.3 Physical Characterisation

When it comes to producing applications containing molecularly imprinted polymer it is not only important to know that they function. What size they are and if they aggregate in different medium or not, thickness of certain layers and surface roughness also become important factors. There is a variety of techniques that can be used for this type of analysis.

Dynamic light scattering (DLS) is a method used to determine for example the size distribution of particles in solution. Particles inside a cuvette scatter light with a wavelength longer than their physical size. Depending on how the particles move in the solution, the resulting intensity of the scattered light will change presented as a correlation value. Larger particles diffuse slower and will have a higher correlation over a longer time. When performing DLS measurements, the refractive index n and the viscosity η of the different solvents are needed.

In electron microscopy the sample is bombarded with electrons of high energy. These will scatter on the sample and by detecting them it is possible to produce images of your samples. There are two main techniques used: scanning electron microscopy (SEM) where the electrons scattered back from the sample are analysed, and transmission electron microscopy (TEM) where the electrons passing through the sample are detected. SEM

instruments are often used for size and geometrical determination of particles, some are however also equipped with X-ray detectors and can be used for compositional analysis as well. TEM instruments are instead used when for example analysing composites such as core-shell structures.

When it comes to analysis of surface structures one possibility is to use atomic force microscopy (AFM). A cantilever is rastered over the surface and the forces acting on it determines the distance between surface and tip. Another surface analysis technique for determination of surface layer thickness is ellipsometry.

2.5 Serotonin Imprinting

Serotonin is a neurotransmitter that can be found in the human body mainly in the gastrointestinal tract, but also in the central nervous system [2, 3]. It plays a great role in many of the bodily functions concerning amongst others mood and hunger. In many of the medications for treatment of depression, anxiety and eating disorders, active substances block the re-uptake of serotonin to the presynaptic neuron causing a higher extracellular concentration. Today the serotonin levels are measured from retrieved blood serum samples.

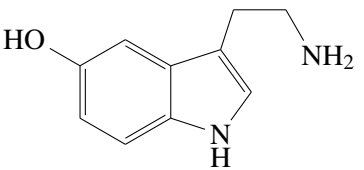

Figure 2.4: *Serotonin.*

2.5.1 Chemical Properties

In the serotonin structure there are two functional groups that are easily ionised, these are the primary amine and the phenolic hydroxyl group [17]. Both groups have pKa values above 9 which results in protonation under neutral pH conditions in aqueous solutions as seen to the left in Figure 2.5. A third group, the secondary amine, also has the possibility to be involved in hydrogen bonding. From proton nuclear magnetic resonance (NMR) measurements these three groups are clearly visible (see Appendix A) and their interactions could therefore easily be monitored by this method.

Serotonin is a redox active compound and is under physiologically relevant conditions electrochemically oxidised at 0.4 V. The proposed two step oxidation scheme is shown in Figure 2.5 [18]. A common issue by the oxidation of serotonin is the formation of serotonin complexes where the molecules interact with one another to form polymeric structures. These then also have a tendency to adhere to surfaces nearby. Serotonin is also prone to auto-oxidation of serotonin is a processes which can be facilitated by high temperature, presence of oxygen or UV-radiation.

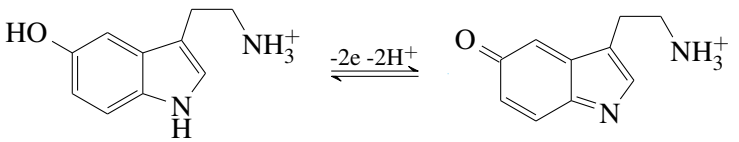

Figure 2.5: *On the left side of the equilibrium is the serotonin in its protonated form. On the other side is the electrochemical oxidation product. The oxidation is a two proton reduction of the molecule.*

Due to its structure: the presence of conjugated double bonds, serotonin is a good auto-fluorophore. The absorption and emission of the molecule is pH dependent but show stable values when the pH is < 8 [17]. The emission maximum is located at 337 nm and the molecule has a clear absorption maximum at 279 nm. The absorption spectrum of serotonin is shown in Figure 2.6.

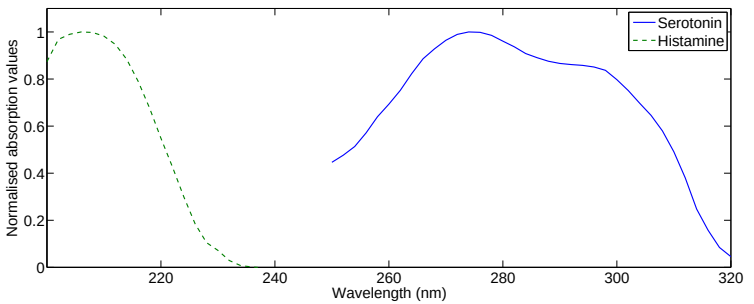

Figure 2.6: *This figure shows the normalised absorption spectra from both serotonin and histamine. Serotonin is dissolved in water and histamine in* 100 *mM PBS buffer, pH* 7.41.

2.5.2 Imprinting Target Groups

The last couple of years some reports of serotonin imprinting have been published [5, 7, 19] with results showing that the polymers are selective for serotonin in buffer solutions. The primary amine and the phenolic hydroxyl group previously mentioned are the main targets of the molecular imprinting process with MAA as the functional monomer. In the prepolymerisation mixture hydrogen bonds between the functional monomer and the template will form. It is also possible for the secondary amine in serotonin to form this type of bond, but due to sterical hindrance the bond will be of less significance.

There are a lot of contradictions in the articles which shows that serotonin imprinting is still in its novel steps. In one case the porogen used for the polymerisation is dimethyl sulfoxide (DMSO) [7], whereas another report on the same topic disregards the same porogen, which due to its high polarity affects the imprinting effect [5]. Also the choices of functional monomers are not regarded equally in the different experiments.

2.6 Histamine Imprinting

Histamine is a low molecular weight biological molecule maybe best known to be involved in immune responses. Histamine is however also present in many foods, generally at low levels, but certain processing methods might increase the concentrations [20]. In many countries histamine levels are regulated due to the risk of toxicity.

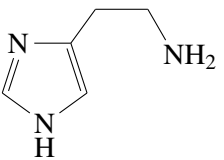

Figure 2.7: *Histamine.*

Analysis of histamine concentration in solutions can be determined with UV-Vis spectroscopy. The absorption of the molecule has a maximum peak around 208 nm which can be seen in Figure 2.6. Due to the low absorption peak there are however limitations to this method. The wavelength corresponds to many other compounds containing a single double bond, for example MAA.

2.6.1 Imprinting Target Groups

The similarity of histamine to serotonin is high as histamine also contains one primary and one secondary amine. Similar imprinting approaches are therefore also utilised. Previous successful imprinting of the molecule has used MAA as the functional monomer [21, 22].

3

Electrochemistry

Electrochemistry is a part of analytical chemistry concerning the connection between chemical reactions and how they are characterised by the movement of electrical charges [23]. These reactions are referred to as reduction-oxidation (redox) reactions and are the basis of the many industries of today. One example is bio-electrochemistry: the analysis of these reactions in biological systems. The fact is that a great deal of biological reactions in nature and in our body simply have to do with electrical charges. Examples are the division of differently charged molecules over neuron membranes and the many coupled processes between molecules and enzymes.

Many different analysis methods have arisen by simply letting these biological reactions occur at an electrode interface in an electrochemical cell [24]. The technique to determine glucose concentrations relies on the interaction between glucose and enzymes immobilised on the electrode. Due to an applied potential on the system a current arises which is detected. This voltammetric approach is one method that is possible to use. Other Electrochemical methods include potentiometry and coulometry, the first analyses a potential between electrodes and the second measures the total charge conducted away from an electrode. The method used in this thesis is a type of voltammetry.

3.1 Voltammetry

The voltammetry method, as previously stated, uses an applied potential which is time-dependent and registers the current which is produced [23]. Different analytes will be oxidised or reduced at different potential values and depending on the direction of potential change. The voltammetric measurement will result in a voltammogram most often displaying the potential versus the current.

Typically a three electrode set-up is used to perform voltammetric measurements. This is schematically shown in Figure 3.1. The set-up consists of three electrodes: the working electrode (WE), the reference electrode (RE) and the counter electrode (CE), and the necessary electrical components to finish the circuit. The reference electrode has a constant potential whereas the working electrode and the counter electrode close the circuit. The interaction with the analyte takes place at the surface of the working electrode. The set-up is connected to a potentiostat applying a variable potential between the working electrode and the reference electrode. This gives rise to a detectable current which can be plotted in a so called voltammogram, an example is shown in Figure 3.2.

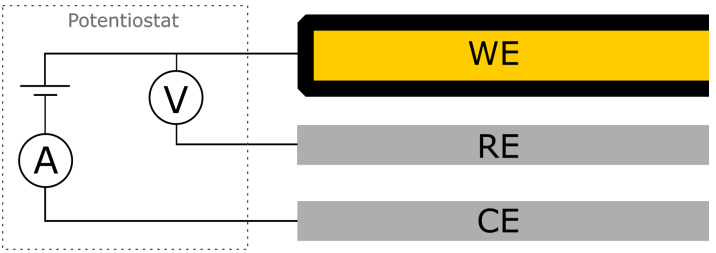

Figure 3.1: *This figure shows a schematic image of a three electrode set-up used for voltammetric measurements. A working electrode (WE), reference electrode (RE) and a counter electrode (CE) are connected to a potentiostat. The potentiostat allows a variable voltage over the WE and the RE which gives rise to a measureable current.*

In a sub-category of voltammetry called cyclic voltammetry, the applied voltage is varied in both positive and negative direction. In this way both the oxidation and the reduction of an analyte showing reversible properties can be represented.

3.1.1 Electrodes

A wide variety of materials can be used for the electrodes. Typical materials for solid working electrodes are platinum or gold [23], both inert and stable materials. A typical counter electrode is a platinum wire and the material chosen for the reference electrode is usually silver chloride. Solid electrodes, in comparison to liquid ones which are sometimes used, have the drawback of unwanted species adsorbing to the surface. The removal of these is nec-

essary for a clear signal and different methods such as mechanical grinding and electrochemical cleaning are used.

An important property of the working electrode is the reaction rate, a parameter highly dependent on the amount of surface atoms in contact with the surrounding medium. The surface of an electrode might be smooth and flat from a macroscopic perspective, but at an atomic level the real surface area is larger due to a more unstructured surface. The reactivity of such an electrode will be higher than that of an atomically flat one. There are many ways to affect the atomic surface area of the electrode, the previously mentioned techniques to remove adsorbed species on the surface also affects the structure. Mechanical polishing usually produces the largest area, whereas chemical polishing instead smoothens out the surface [25]. The roughness factor R_f is calculated by dividing the real surface area with the projected geometric area.

For a gold electrode in sulphuric acid, an oxide layer will form on the surface. Due to the oxidation of the acid this is assumed to consist of one oxygen atom per surface gold atom. The total charge amount adsorbed will then correspond to the real surface area of the electrode. Equation 3.1 provides a method to calculate the real surface area (A) from the total adsorbed charge (Q), and the reference charge (Q_{ref}).

$$Q = 2\,e\,N_A\,\Gamma A = Q_{ref}\,A \tag{3.1}$$

The reference charge (Q_{ref}) depends on the amount of oxygen atoms adsorbed to the surface (Γ), Avogadro's number (N_A) and the elementary charge (e) are constants. The amount of oxygen was, as previously stated, assumed to equal that of metal atoms at the surface. This value will however strongly depend on the crystallographic orientation of the metal. For polycrystalline gold electrodes this value is approximated to 390 $\mu C\,cm^{-2}$. The total adsorbed charge (Q) can be calculated from the voltammogram by integration the current of interest. The voltammogram in Figure 3.2 shows one cyclic scan of a gold electrode prepared to have a very large real surface area, sometimes referred to as 3D electrode [26]. The peak labelled B is assumed to represent the full reduction of the gold electrode, integration of this peak will give Q for the reduction.

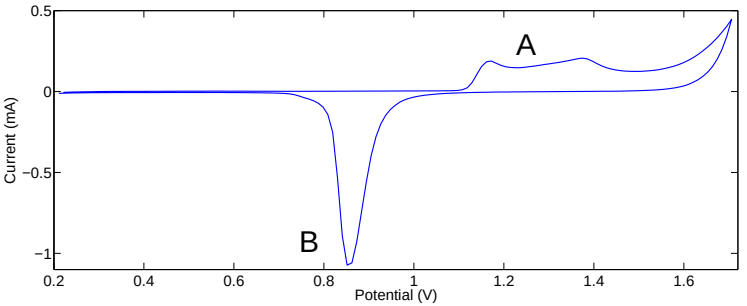

Figure 3.2: *This figure shows one scan of a cyclic voltammetry measurement of a gold 3D electrode in H_2SO_4. The positive peak A arises due to oxidation of the acid, wheras B represents the reduction. The peak at the highest voltages is due to surface oxidation of the gold electrode.*

3.1.2 Currents

Different currents arise in the system and these are usually divided into two categories: faradaic and non-faradaic currents. The faradaic currents are the currents created due to the redox reaction. Depending on the nature of the reaction, the current produced will flow in different directions. A negative (cathodic) current is produced when the analyte is reduced. The opposite applies to the anodic current or the analyte oxidation. Non-faradaic currents arise from the movement of charges due to the change of potential, and from residual molecules in the system. Reference measurements without the analyte will provide information of these non-faradaic currents to differentiate them from the redox dependent.

3.1.3 3D-Structured Electrodes

As mentioned before the reaction rate of the system is dependent on the real electrode surface area. A way to increase this is by the means of permanent immobilisation of gold nanoparticles (AuNP) on the surface [26]. The AuNPs are synthesised by the reduction of a gold salt. A concentrated dispersion of the particles are then dropped on the electrode and let to dry. The electrode is submitted to electrochemical cleaning by cyclic voltammetry in sulphuric acid. The particles on the surface will grow into one another a therefore be stabilised on the surface increasing the surface roughness.

4

Experiments and Results

This part of the thesis presents the methods used for the different experiments and the results produced. The work is divided into two different main stages: the polymer synthesis and the electrochemistry, this is also the order in which they are represented. Because the different stages are covering different fields the results of each stage will be presented before the method for the next begins.

Characteristic values of chemicals and solvents for calculations have been found in the Solvent Center by Sigma-Aldrich [27] and are valid at room temperature and all graphs have been plotted with MATLAB R2014A unless otherwise stated.

4.1 Presynthesised Particles

The first stage of the thesis work was to analytically characterise already existing MIP nanoparticles. The particles had been synthesised by Sudhirkumar Shinde, postdoctoral researcher in Börje Sellergren's team at Malmö University. One of the three different protocols used was based on work prepared by Reza Mohammadi, previously a PhD student in the same group. The characterisation methods used were HPLC and fluorescence spectroscopy for analytical equilibrium rebinding tests and DLS measurements for physical properties.

4.1.1 Protocols

All three polymers had been synthesised on 20 nm silica beads through RAFT polymerisation. The silica particles had been aminofunctionalised and terminated by the RAFT agent 4-cyanopentanoic acid dithiobenzoate (CPDB), then initiated thermally and using the initiator 2,2'-azobis(2,4-dimethyl valeronitrile) (ABDV), polymerisation took place at 50 °C for 20 h. The

cross-linker ethylene glycol dimethacrylate (EGDMA) was used for all three polymers and the initiator:RAFT ratio was 1 : 3.

The polymers and their different protocols will from now on be referred to with the numbers $1-3$.

The first protocol used vinylsulfonic acid sodium salt solution 25% in H_2O as a functional monomer and toluene as a porogen. The second and the third protocols used both methacrylic acid (MAA) and methacrylamide (MAam) as functional monomers. Dimethylformamide (DMF) was used as a porogen in protocol two whereas toluene was used in protocol three.

4.1.2 Equilibrium Rebinding Tests

For the analytical characterisation equilibrium rebinding tests were performed. 10 mg of material was weighed and to that 1 mL of a known concentration template-solvent combination was added. The system was shaken during a certain amount of time before centrifugation. 200 µL of the supernatant was transferred to either a 96-well plate or HPLC vials. Equilibrium time was somewhat varying, but generally the samples were left over night for a minimum of 10 h.

To be able to calculate the concentrations of analyte in the supernatant, calibration curves were retrieved by preparing different concentrations of the template in the solvent used for rebinding tests. Mean values of two to three measures were plotted, and a linear regression was calculated to retrieve the equation of the linear function.

4.1.3 RP-HPLC Analysis

Two different methods were used. In both cases the rebinding solvent used was a mixture of acetonitrile and water (MeCN:H_2O 99 : 1). The samples were centrifuged after 23 h and the supernatant was transferred to HPLC vials. RP-HPLC was performed on the vials. The mobile phase in the first method was prepared according to a protocol by Xiao et al. [28]. A flow rate of 1 $\mathrm{mL\,min^{-1}}$ was used, the maximum pressure set to 130 bar and the volume of the extracted aliquots was 20 µL. The chromatograms were analysed at 275 nm. The second HPLC method used followed the protocol by [29], with a mobile phase consisting of a 5 mM phosphate buffer containing 3% methanol. All other parameters used were the same.

The equipment used was an ALLIANCE WATERS 2695 SEPARATIONS MODULE in combination with a WATERS 2996 PHOTODIODE ARRAY DE-

TECTOR, utilising a PHENOMENEX LUNA 250mm×4.6mm coloumn packed with 5 µm porous silica beads coated with C18.

4.1.4 Fluorescence Spectroscopy

Fluorescence analysis was performed on the supernatant after equilibrium rebinding tests and the particles were centrifuged. A 96-well quartz plate was read in a GEMINI EM MICROPLATE READER in top mode. The excitation wavelength was set to 270 nm and the emission was measured at 336 nm.The rebinding was performed in three different solutions: water, 150 mM PBS with 50 mM saline and in a mixture of methanol and acetic acid in the ratio 99 : 1. Calibration curves were retrieved for all three solvents, and the free and bound concentrations of the analyte were calculated.

4.2 Bulk Polymerisations

A couple of different batches of bulk polymer with different templates were prepared. The different batches are presented in Table 4.1. Elaborate descriptions of the protocols will follow in this section.

Table 4.1: *This table presents the different batches of polymer prepared and analysed during the project. The templates used were either Ser (serotonin) or Hist (histamine). Some of the differing properties of the batches are also presented. For every batch a NIP was produced following the same recipe.*

Batch	T	Protocol	Comments
MIP2	Ser	Peeters et al. [7]	Thermal and photo initiation.
MIP3	Ser	Peeters et al. [7]	–
MIP4	Ser	Peeters et al. [7]	Prepared without cooling.
MIP5	Ser	Peeters et al. [7]	Prepared at room temperature.
HMIP1	Hist	Horemans et al. [22]	–
HMIP2	Hist	Foteini et al. [21]	$CHCl_3$ and EGDMA
HMIP3	Hist	Foteini et al. [21]	$CHCl_3$ and EGDMA
HMIP4	Hist	Foteini et al. [21]	MeCN and EGDMA
HMIP5	Hist	-	Core-shell $CHCl_3$

4.2.1 Serotonin Imprinting

A protocol produced by Peeters et al. [7] was followed for the preparation of MIP2-5. The following values represent one sixth of the original protocol. 0.47 mmol of MAA, 1.4 mmol acrylamide (AM), 3.8 mmol EGDMA and 0.95 mmol serotonin hydrochloride were dissolved in 1.2 mL dried dimethyl sulfoxide (DMSO). The initiator azobisisobutyronitrile (AIBN) was added (0.10 mmol) and the mixture was shaken a couple of minutes. The solution was purged under nitrogen for 10 min before transferred to glass NMR tubes, that were sealed.

The polymerisations were initiated by UV light, except one part of MIP2 which was initiated thermally. For photoinitiation the NMR tubes were placed in a UV cabinet (15 h). Thermal initiation took place in an oven set to 65°C for a total time of 19 h. The polymers were retrieved from the NMR tubes and mechanically ground in a mortar and pestle. For all serotonin batches the MIP showed a clear yellowish color visible in Figure 4.1a. This non-white color was later assumed to indicate the oxidation of the template molecule.

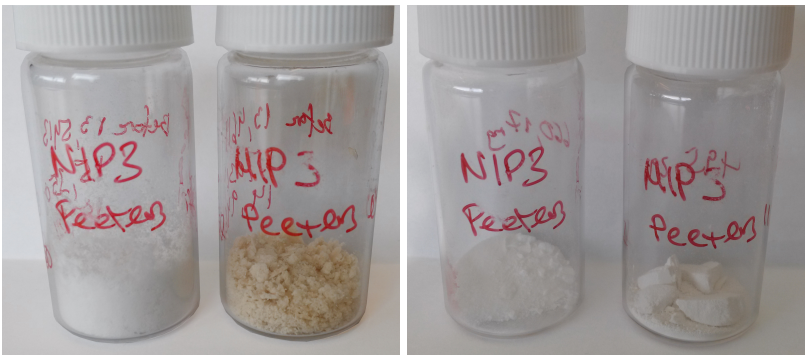

(a) *MIP3 before washing.* **(b)** *MIP3 after washing.*

Figure 4.1: *The two images show the visual difference of the photoinitiated polymers before and after washing. Image **a)** shows them before washing and image **b)** is after. There is a clear color change from brownish yellow to white for the MIP.*

The UV polymerisation set-up used consisted of a self constructed cooling system in combination with a commercially available UV source. The cooling system utilised a JULABO FT401 immersion cooler put in the bath

of a JULABO 5B UC circulator thermostat to reach a temperature of ± 0.6 °C. To the circulator one straight condensers was connected inside which the NMR tubes were put. The condenser was approximately 10 cm from the UV source of a commercially available nail curing lamp YF 7272, with an emission peak at 365 nm. The intensity at the polymerisation distance was measured with a SPER SCIENTIFIC UV LIGHT METER. The absorption of UV light by the glassware was measured whereas the absorption by water was assumed to be negligable [30].

To remove the template and other unwanted molecule residues, for example oligomers, the polymers were washed. Both the MIP and the NIP particles were subjected to the same washing procedure. For MIP2 the procedure used differs from the synthesis protocol. Instead of using a Soxhlet set-up the polymers were immersed in the washing solution. The test tubes were put on a rotator for one hour and after this centrifuged for 15 min at 4000 rpm. The washing solution was replaced and the procedure repeated. Fluorescence spectroscopy was used to analyse the supernatant to monitor the washing. The first washing step took place in pure methanol. This was followed by two washing steps with MeOH:formic Acid:H_2O (80 : 15 : 5). This was followed by four steps of washing in MeCN:acetic acid (1 : 1). After the washing the particles were dried over night in an oven at approximately 40 °C.

MIP3 was washed according to protocol. MIP4 and MIP5 were washed with the same amount of washing cycles as MIP2, but using the same solvents as in the protocol, that is a 1 : 1 mixture of AA and MeCN. Rebinding tests were prepared with an equilibration time of 2 h in milliQ-water, and analysis was done with flourescence spectroscopy using the same parameters as in Section 4.1.4. Due to small batch sizes of MIP4 and MIP5 only two concentrations could be analysed simultaneously.

4.2.2 Serotonin Purity measurements

As will later be discussed, there were thought that there was too high concentration of oxidised serotonin in the synthesised polymer. An initial thought was that the intensity of the UV light was too high. Therefore proton NMR measurements were performed on both non-oxidised serotonin in deuterated DMSO, as well as a mixture of serotonin in deuterated DMSO that had been subjected to the UV light for 15 h.

4.2.3 Histamine Imprinting

A protocol produced by Horemans et al. [22] was followed. The values following represent one seventh of the originial protocol. 2.5 mmol of MAA and 1.2 mmol of histamine was dissolved in 1 mL of DMSO, the mixture was well shaken. 5.1 mmol of EGDMA and 94 µmol of the initiator AIBN was added. The mixture was then purged in nitrogen for approximately 5 min. The vials was sealed and placed in a thermostatic bath set to 65 °C for 12 h.

A second histamine protocol, derived from work by Trikka et al.[21] was followed. The same molar ratio, 0.8 : 4 : 20 for T:M:CL was used, but instead of using AIBN as the initiator ABDV was used. As stated in Table 4.1 EGDMA was used as a cross-linker and both batches with $CHCl_3$ and MeCN as porogens were produced. HMIP2 was synthesised by the laboratory supervisor Sudhirkumar Shinde, whereas batches HMIP3-5 were synthesised by myself.

The washing procedure was the same one used for serotonin, but the solvent now limited to a mixture of methanol and acetic acid (9 : 1) for all the batches. The supernatant was collected from every washing step to perform quantitative analysis of analyte removal. Rebinding tests of the histamine bulk MIPs were all performed in a PBS 50 mM solution with an equilibration time of 4 h followed by analysis with UV-Vis spectroscopy measuring absorbance at 208 nm. Measurements were performed on a BIOTEK POWERWAVE XS plate reader in a 96-well quartz plate.

4.2.4 Histamine MIP Cross-Reference

Serotonin was chosen as an analyte with which to perform cross-reference rebindning tests. The batch HMIP3 was subjected to this test. The bound concentrations of either histamine or serotonin were measured as previously stated. The supernatant was thereafter completely removed. 1 mL of a PBS:MeCN mixture 9 : 1 was added, to remove the non-specific binding on the polymers. The suspension was shaken for 4 h followed by centrifugation. Analysis was performed by fluorescence spectroscopy or UV-Vis spectroscopy in accordance to previous methods.

4.2.5 Histamine Core-Shell MIP Nanoparticles

For the final batch produced, the protocol from batch HMIP3 was applied on a core-shell structure. Silica nanoparticles (SiNP) wih a size of 200 nm were aminofunctionalised according to the protocol by Mohammadi [15]. After

that the SiNP-NH was terminated with RAFT agents to be ready for further polymerisation. 1.38 mmol of the RAFT agent CPDB, ethyl chloroformate ($C_3H_5ClO_2$) and triehylamine (TEA) were dissolved in 50 mL tetrahydrofuran (THF) in a three-necked round bottom flask. After nitrogen purging the mixture was kept at -67 °C for 40 minutes under stirring. 7 g SiNP-NH was added and the stirring was kept over night. The mixture was precipitated twice in hexane before left to dry in room temperature.

800 mg SiNP-NH-RAFT particles were dispered in of chloroform. A homogenizer was used, and the solution was sonicated for 30 min to try to reach monodispersion. In a seperate vial histamine (T) together with MAA and EGDMA (M and CL) were dissolved in chloroform. The two mixtures were combined to a total volume of 20 mL chloroform and purged under nitrogen for 20 min. The initiator ABDV was added and the mixture was once again purged for 20 min before put on a heated shaking plate, 50 °C for 22 h.

4.3 Serotonin MIP Results

4.3.1 Synthesis and Preparation

A total of five batches of serotonin MIPs and NIPs were prepared but only batches MIP2-5 were submitted for evaluation. Unfortunately with no imprinting effect present. Material yield was estimated only for MIP3 to approximately 84.5%. During the first washing step it was also noticed that the vials used for washing were not completely sealed and therefore the value could be slightly misleading. MIP2 could not be analysed at all, due to the fact that it was not completely polymerised. Transfer to NMR tubes were done with disposable non-graded pasteur pipettes, and the constituents in the vial was not polymerised. For batches MIP4 and MIP5 the main goal was to perform quick testing and the total mass of polymer was not registered.

The intensity of the UV light was measured at the approximately same distance at which the polymerisation took place. Since the detector did not fit inside the condenser tube one measurement was performed with an empty condenser tube carrying an empty NMR tube inside, $I_{cond} = 6.56\ \mathrm{mW\,cm^{-2}}$. A second measurement was performed without anything between the detector ant the UV source, $I_0 = 7.63\ \mathrm{mW\,cm^{-2}}$. The intensity at the polymerisation center was therefore calculated to approximately $7.1\ \mathrm{mW\,cm^{-2}}$. Half the difference between I_{cond} and I_0 equals to the middle of the condenser.

Images were taken of the batches before and after polymersation. In Figure 4.2 the prepolymerisation mixtures of two NIPs and two MIPs are shown. In this case, as for all batches, the MIP showed a distinct pinkish color showing the prescence of oxidised serotonin. The images in Figure 4.3 shows batch MIP5 before and after polymerisation. In Figure 4.3a the color of the MIP (left) is not as distinct as in Figure 4.2, mainly due to a smaller batch size but also to more precautions taken. Figure 4.3b shows a dark brown color of the MIP, also this due to oxidised serotonin present. This color disappered during washing as seen in Figure 4.1b.

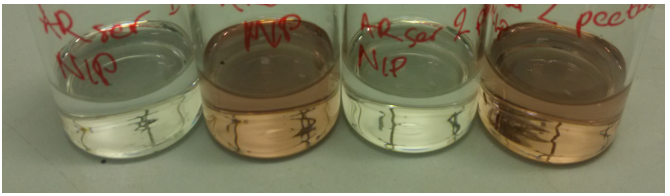

Figure 4.2: *This image shows the prepolymerisation mixtures of two serotonin batches. The clear color difference exists between the NIP mixtures (transparent) and MIP mixtures (pink). The color is due to the prescence of oxidsed serotonin.*

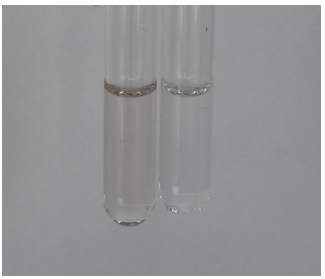

(a) *MIP5/NIP5 before polymerisation.*

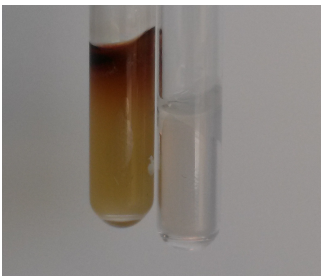

(b) *MIP5/NIP5 after polymerisation.*

Figure 4.3: *The two images shown in **(a)** the prepolymerisation mixture of MIP5/NIP5 (in written order). In **(b)** are the same NMR tubes after photoinitiated polymerisation. The MIP has gone through a clear color change from very slightly pink to very brown, which is a sign of oxidised serotonin.*

Washing curves to monitor the removal of template from polymer were

produced for MIP2. These are presented in Figure 4.4. No quantitative information was retrieved from these polymers.

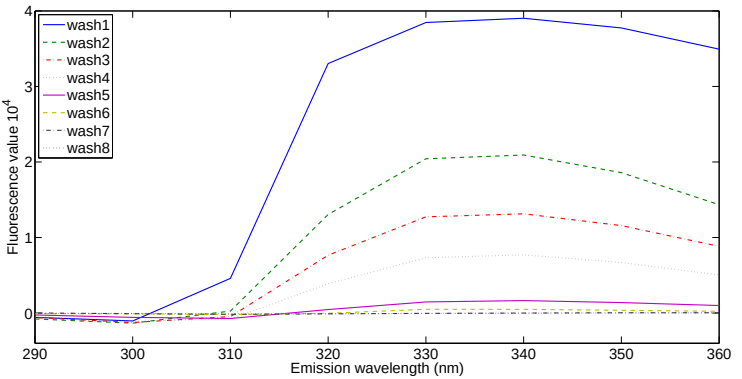

Figure 4.4: *This graph shows how the concentration of serotonin in the supernatant decreases until it can be assumed zero during the eight washing cycles performed. Wash 1 took place in methanol,wash 2 and 3 in methanol:formic acid:water (80:15:5). Wash 4 was performed in methanol due to storage over night. The final four washes, 5-8 took place in MeCN:acetic acid (1:1). After washing the particles were rinsed with methanol to remove the acid residues. Fluorescence emission was measured between* 290 *and* 360 nm *after excitation at* 270 nm

4.3.2 Rebinding

To be able to analyse the supernatants from the rebinding tests and calculate the analyte concentrations, standard calibration curves for every analyte-solvent combinations and for the different analytical methods had to be calculated. Figure 4.5a shows the result for serotonin in water. The linear region lies between $0.1 - 10$ µM. Values of the coefficient of determination was calculated to $R^2 = 0.9961$ for serotonin.

Rebinding analysis of the presynthesised MIP particles in three different solvents were prepared. The results (not shown) did not show any sign of functioning MIPs. There was no difference between MIP and NIP particles.

Rebinding experiments of the bulk polymerised serotonin MIP were carried out in water, according to protocol. 18.1 wt% template was used during the synthesis. This means that the highest possible capacity of the polymer is approximately 1 $\mathrm{mmol\,g^{-1}}$. The binding isotherms represented in

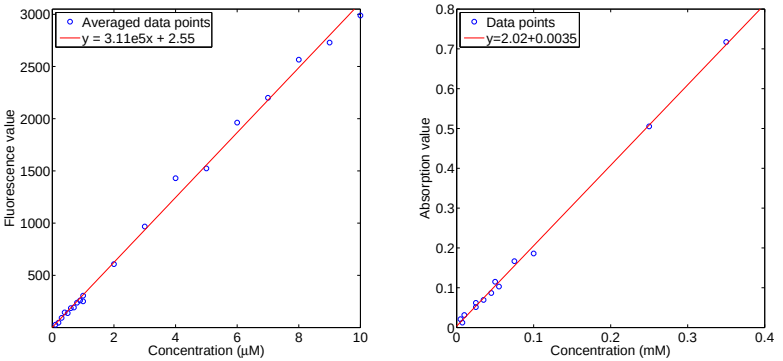

(a) *Standard calibration curve for serotonin in H_2O.*

(b) *Standard calibration curve for histamine in PBS* 50 mM.

Figure 4.5: *The graphs show the standard calibration curves for serotonin in water* ***(a)*** *and for histamine in PBS* 50 mM ***(b)***. *The respective* R^2 *values are* 0.9961 *and* 0.9981.

the followd protocol showed bound concentrations in the range of $30 - 150$ $\mu\text{mol}\,\text{g}^{-1}$ for the used concentration interval.

Only the graphs from batches MIP4-5 are shown (Figure 4.6) where the weight-normalised bound concentration of analyte is plotted versus the free concentration in the supernatant. The results for all the batches were similar: rather low values of bound analyte and no difference between MIP and NIP. This indicates that the particles exhibit some amount of non-specific binding, but probably low or none specific binding.

4.3.3 Serotonin Purity Studies

NMR spectra of both fresh serotonin and serotonin subjected to UV light are shown in Appendices A and B. The characteristic peaks of the hydrogen atoms number 8, 7 and 13 are visible in both of the spectra which indicates that there is still non-oxidised serotonin after UV illumination. If only oxidised serotonin was left, at least the peak for hydrogen number 7 would no longer be visible.

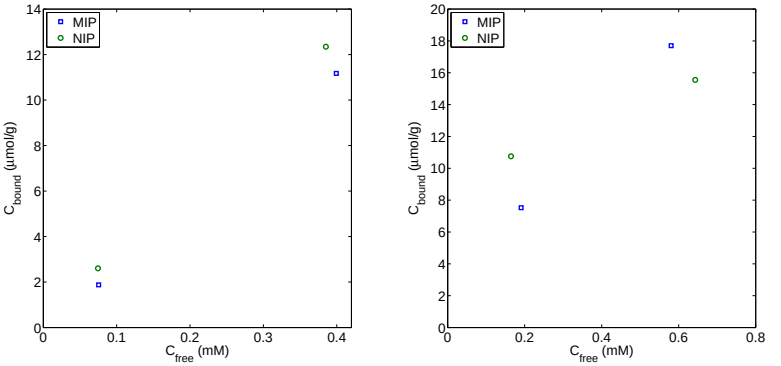

(a) *Rebinding of MIP4 in H_2O* **(b)** *Rebinding of MIP5 in H_2O*

Figure 4.6: *Rebinding graphs of MIP4-5 in H_2O. Both batches were prepared under different temperature conditions than the protocol suggested. Due to small batch sizes only two concentrations could be submitted for rebinding.*

4.4 Histamine MIP results

4.4.1 Synthesis and Preparation

A total of five batches of histamine MIPs were synthesised where HMIP1 and HMIP3-5 were prepared by myself. Therefore the analysis of HMIP2 is not mentioned in this section. The yields for all the histamine MIP bulk batches were calculated with a mean value of 91.7%

Histamine is a molecule which does not oxidise as easily as serotonin. This does however not exclude that there still might be oxidation. In Figure 4.7a the MIP has turned yellow signalling the presence of oxidised histamine. This color change is not visible in the comparison between MIP and NIP for batch HMIP4 in Figure 4.7b.

For the histamine batches HMIP3-4 the washing solvent was collected and analysed to calculate the total amount of analyte removed. The calculated value reached approximately 4.6 g which would correspond to 17000% of the starting concentration. This value, of course not reasonable, can be explained by the high absorption of many compounds at the short wavelengths used.

4.4.2 Rebinding

The rebinding results of batch HMIP1 did not show any sign of imprinting (not shown). Batches HMIP2-4 all did show imprinting properties. Since HMIP2 did show binding results, the subsequent batches were produced. Rebinding data from HMIP4 was compared to that of HMIP3, and from this was concluded that the difference between MIP and NIP was higher for HMIP3. This is why this batch was chosen for further analysis. There is a significant difference in the bound amount of histamine to the MIP particles in comparison to the NIP particles.

The amount of histamine used during the synthesis was 2.07 wt% template. This corresponds to a possible maximum binding capacity of approximately 180 $\mu mol\,g^{-1}$.

A fit was made to the binding data of both the MIP and the NIP using a heterogeneous binding model considering the whole concentration spectrum. The data and the fitted curves are shown in Figure 4.8. The number of binding sites N is calculated to approximately 50 $\mu mol\,g^{-1}$ and the average binding affinity K_d to 0.61 mM. Calculations and plots were prepared using the GRAPHPAD PRISM 6 demo software.

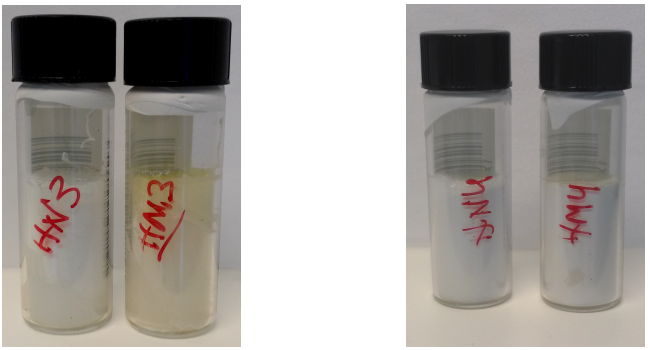

(a) *HMIP3/HNIP3 after polymerisation.*

(b) *HMIP4/HNIP4 after polymerisation.*

Figure 4.7: *This figure shows the batches HMIP3* ***(a)*** *and HMIP4* ***(b)*** *after polymerisation. A difference in color is visible between MIP and NIP for batch HMIP3. This yellow color is due to the presence of oxidised histamine. For batch HMIP4 there is no visible color difference.*

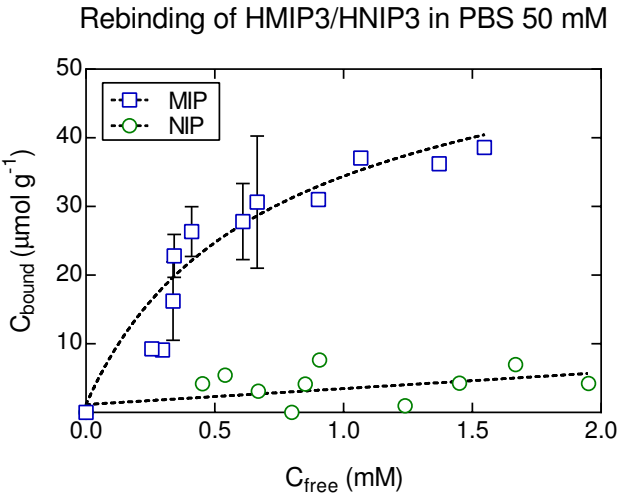

Figure 4.8: *This graphs shows the rebinding curves of HMIP3 in PBS* 50 mM *fit to a homogeneous binding model. The fit is used to calculate values for number of binding sites and binding affinity. Error bars are shown where triplicate measurements were performed.*

4.4.3 Cross-Reference Rebinding

In Figure 4.9 results from a cross-reference rebinding test for HMIP3 is shown. The particles were tested with serotonin, since it has a similar structure, and already played a big role in the project. The data points were measured at an initial concentration of 1 mM of the analyte. Two washing steps in a 9 : 1 mixture of PBS and MeCN followed where the amount of analyte still bound to the particles were analysed. As can be seen the binding of serotonin to the polymer is a lot higher than the histamine binding. Both analytes are also washed away in a similar pace.

4.4.4 Histamine Core-Shell MIPs

The material yield was calculated to 93% for the process of RAFT termination, whereas for the polymerised MIP and NIP particles only a mean yield of 68% was reached, which is low, but not the greatest care was taken to not lose material at this point. The particles were subjected to a equilibrium rebinding test without any sign of imprinting.

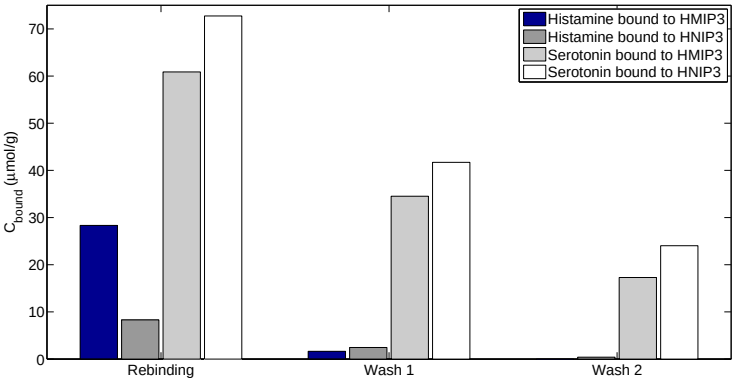

Figure 4.9: *This graph shows the results from the cross-reference binding test performed on HMIP3/HNIP3. At a first step histamine and serotonin where bound to the polymers with an initial analyte concentration of* 1 mM. *Two washing steps followed using a 9:1 mixture of PBS:MeCN and the bars shown represent the amount of analyte still bound to the specific particle.*

4.5 Electrochemistry

The start of the project involved electrochemistry. A simple approach was tried where the MIPs was incorporated in the synthesis of a highly structured three dimensional surface. The hope was to see a variation in signal depending on the serotonin concentration. Gold nanoparticles were to be synthesised and analysed. These would then be merged into the electrode surface to create the highly structured 3D electrode. The surface area would be determined through measurements and calculations. Finally the immobilisation of the MIPs would take place for cyclic voltammetry measurements.

All electrochemical measurements were performed with the three electrode set-up explained in Section 3.1. The working electrodes that have been used are circular gold electrodes from BIOANALYTICAL SYSTEMS with a geometrical surface area of 3.1 mm^2. As a reference an Ag/AgCl electrode (3M KCl E= 0.210 V versus standard hydrogen electrode) has been used and a coiled platinum wire as a counter electrode. The utilised potentiostat was a μAUTOLABIII/FRA2 impedance analyser and the electrolyte used a 50 mM phosphate and 150 mM saline PBS buffer, pH= 7.41 unless stated

otherwise. All measurements shown including MIP or NIP particles were performed on particles synthesised from Protocol 2.

4.5.1 Gold Nanoparticle Synthesis and Characterisation

AuNPs with the size of 20 nm had to be prepared for 3D electrode synthesis. A slightly modified version of a citrate gold reduction from Grabar et al. [31] was followed. A 50 mL, 1 mM solution of Gold(III) chloride trihydrate ($HAuCl_4 \cdot 3\,H_2O$) was prepared and heated to 90 °C during stirring on a hotplate. A 1 wt% solution of sodium citrate dihydrate ($Na_3C_6H_5O_7 \cdot 2\,H_2O$) was prepared and 4.4 mL were added to the gold solution. The mixture was kept at 90 °C and under stirring for 15 min. The stirring was then switched off and the mixture was left for 10 min at a constant temperature before it was cooled down. The solution was centrifuged at 10000 rpm for 30 min, 98 % was assumed supernatant and removed. The particles were collected and stored in a fridge before further analysis.

The correlation between concentration and size of gold nanoparticles to the spectra obtained by UV-Vis measurements has been determined by Haiss et al. [32]. By performing UV-Vis measurements on the AuNP dispersion and comparing the absorption at the surface plasmon resonance peak with the absorption at 450 nm the size of the particles can be determined. From the size the concentration can be calculate. For this the tables in the supporting information to [32] were used.

The gold nanoparticles were analysed in a SHIMADZU UV-1700 PHARMASPEC UV-Vis spectrophotometer. A first try of a 1 : 5 dilution showed a too high absorption. Further on dilutions of 1 : 30, 1 : 50, 1 : 100 and 1 : 200 were prepared, the last two giving absorption values lower than 1.

3D Electrodes

The method of synthesising 3D electrodes used has been reported by Andorolov et al. [26]. AuNPs with a diameter of 18 nm were cast on the electrodes three times at a volume of 3 µL. After drying, the electrodes were electrochemically washed in 0.5 M sulphuric acid (H_2SO_4) by 5 cyclic voltammetry scans between 0.2 and 1.7 V, the scan rate used was 100 $mV\,s^{-1}$. An image of one of the two gold electrodes used can be seen in Figure 4.10. The electrodes were finally rinsed with milliQ-water. Before any new measurements the bare gold electrodes were polished with an aluminium slurry (0.3 µm) and rinsed and sonicated in milliQ-water. The electrodes were characterised by analysis of the acquired voltammogram.

Numerical integration of the gold reduction peak was performed to calculate the active surface areas and the roughness factor of the electrodes.

Reference measurements were performed to compare the serotonin oxidation in PBS buffer at both bare gold electrodes and at 3D-structured electrodes.

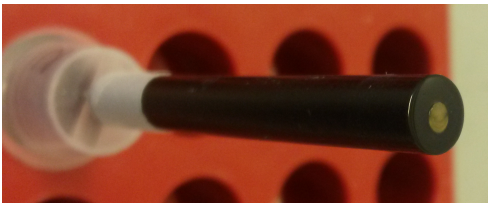

Figure 4.10: *The image shows one of the two identical gold electrodes used during all the electrochemical measurements. Gold nanoparticles have been dropped on the gold surface and let to dry.*

4.5.2 CV Measurements

Mixtures of AuNPs and MIP or NIP particles were prepared with an approximate weight ratio of 1 : 1. A total of 6 µL of this dispersion was cast on the gold electrode. The electrodes were then submitted to the procedure for producing 3D structures mentioned in the previous section. The electrodes were rinsed very carefully in milliQ-water. Cyclic voltammograms were collected for the electrodes in both pure PBS solution and in a PBS solution containing 160 nM serotonin. The method used consisted of three cyclic scans from 0.2 to 0.6 V with a scan step of 10 $\mathrm{mV\,s^{-1}}$.

4.6 Electrochemical Results

4.6.1 Gold Nanoparticles

The UV-Vis absorption spectrum performed on the gold nanoparticles for two different dilutions are presented in Figure 4.11. These both show clear absorption maxima at 522 nm, previously referred to as the surface plasmon resonance peak. Their respective absorption values A_{spr}, and the values at 450 nm A_{450} are presented in Table 4.2. Also represented are the values extracted from the supporting information to [32] regarding particle diameter and concentration. The diameter was determined to 12 nm and the con-

centration of the non-diluted dispersion was calculated to approximately 0.6 µM.

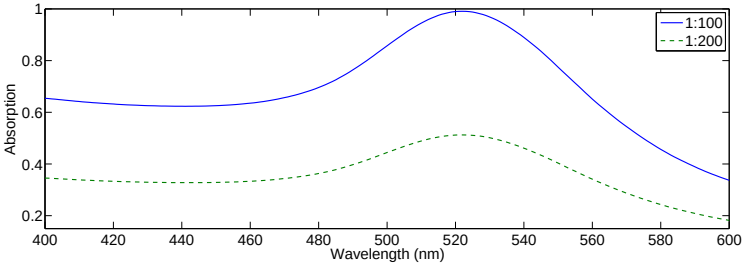

Figure 4.11: *This graph shows the absorption values versus the wavelength for two dilutions of colloidal gold in aqueous solution. The information was used to calculate the approximate diameter and concentrations of the synthesised gold nanoparticles.*

Table 4.2: *This table shows the values from the UV-Vis measurements performed to determine the size of the gold nanoparticles. The dilution factor of the suspensions, the wavelength of the SPR peak, the absorption value at SPR, the absorption value at* 450 nm *and the approximated values of the particle diameter and the particle concentration.*

Dilution factor	λ_{spr} (nm)	A_{spr}	A_{450}	Dia. (nm)	Conc. (µM)
1 : 100	522	0.9907	0.6255	12	0.57
1 : 200	522	0.5123	0.3285	12	0.60

4.6.2 Real Electrode Surface Area

For the determination of the real surface area of the electrode the scan in Figure 3.2 is used. It shows the final out of five scans of the electrochemical cleaning process. The integrated value of the peak was approximately determined to -92.75 µC. By using Equation 3.1 and the approximated value of Q_{ref} for gold (390 µC cm^{-2}) the real surface area could be calculated to 2.4 cm^2. This can be compared to the geometrically visible surface area which was measured to 3.1 mm^2. The active surface area of a bare gold electrode was calculated to approximately 9.6 mm^2. Roughness factors were calculated to approximately 80 for the 3D-structured electrode and 3 for the bare gold electrode.

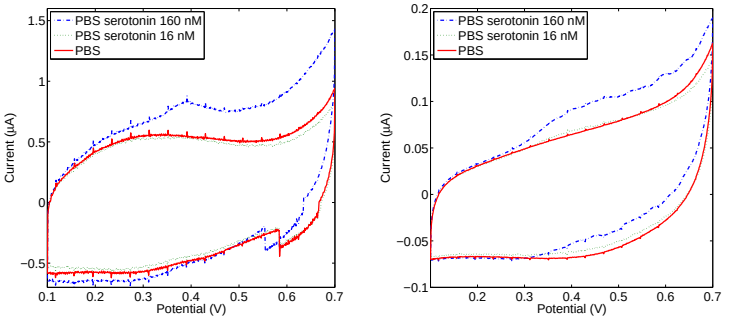

(a) *3D-structured electrode.* **(b)** *Bare gold electrode.*

Figure 4.12: *These graphs show the different voltammograms of serotonin oxidation at 3D-structured gold electrodes* ***(a)*** *or bare gold electrodes* ***(b)****. Each measurement consisted of three cycles, the third are shown.*

The comparison between the 3D-structured electrodes and a bare gold electrode is shown in Figure 4.12. Serotonin oxidation can be seen at 0.4 V due to the increased current. The lack of a reduction peak indicates that the oxidation is irreversible. Higher currents on the 3D-structured electrode correspond to the larger active surface area. The reason as to why the 3D-structured shows a peak at 0.4 V and not a permanent current increase as for the bare gold electrode, is due to diffusion limitation. The graphs also show that detection down to concentrations at 160 nM with both these systems are possible, whereas 16 nM is not distinguishable.

4.6.3 CV Measurements

The measurements with immobilised particles on the 3D-structured electrode surface are shown in Figure 4.13. Measurements were first performed in the PBS solution not containing serotonin before the serotonin measurements. Plotted is the third out of three scans. The two electrodes with immobilised particles show a lower current than the reference measurement confirming a lower active surface area. How this coverage looks would need further investigation. In all three measurements the measurement in PBS with serotonin result in a lower current than the measurements in pure PBS, and in the specifically shown graphs the difference in current is greater for the MIP prepared electrode than for the NIP prepared electrode. Those results were however not reproducible.

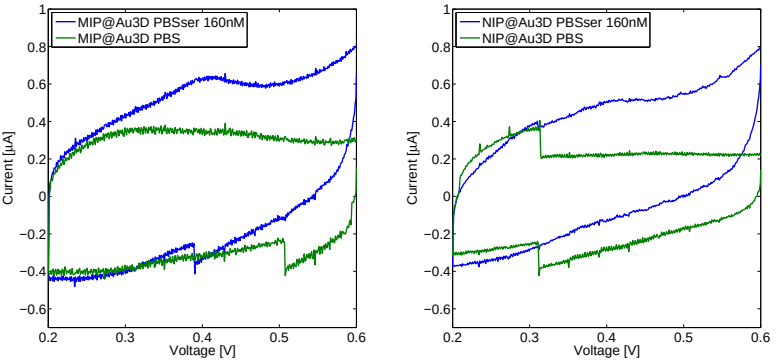

(a) *MIP electrode.* **(b)** *NIP electrode.*

Figure 4.13: *The graphs show CV measurements in both pure PBS and PBS with* 160 nM *serotonin.* ***(a)*** *uses a 3D-MIP electrode and* ***(b)*** *a 3D-NIP electrode. The showed scans are the third and last one for each measurement. Serotonin is clearly detected at* 0.4 V.

5

Discussion

5.1 Electrochemistry on Presynthesised MIPs

The polymer particles used for the electrochemical measurements had been synthesised by Sudhirkumar Shinde according to the protocols in Section 4.1.1. Protocol number 1 had also previously been synthesised within the research group and had shown promising results, unfortunately not available. This part did however suffer from some miscommunication between student and supervisor. The pre-synthesised particles had not yet been functionally tested, which of course should have been the basis of at all going into the electrochemical measurements. It did turn out that the particles did not function which could have easily have been visually characterised. RAFT polymerised particles that work display a pink color from the RAFT agent, which the tested particles did not. Nevertheless, the discussion on the electrochemical part is mainly based on the assumptions that the particles did work.

The first step of this electrochemical part was to synthesise and analyse gold nanoparticles. These would be dispersed together with the MIP particles and then cast onto a gold electrode. Through chemical cleaning a 3D-structured surface would be synthesised. The hope was that the incorporated MIP particles in the surface would accumulate a higher local concentration of serotonin at the surface visible by a higher current at the oxidation peak in amperometric measurements.

The reason for using gold electrodes in the system is not obvious. They are expensive and they do not show the highest sensitivity. This decision mainly relied on the argument that they are good for learning. In my case, I am not that familiar with electrochemical measurements, but gold electrodes have been around for a long time and the amount of literature on how to perform calculations is large. Therefore, a simple proof of concept could be

prepared with gold electrodes, but for a future product a different material would probably be used. Also amperometry was decided on mainly because of it being a simple technique to learn, in the short time I was going to work with the project.

5.1.1 Gold Nanoparticle Synthesis and Characterisation

Synthesis of the gold nanoparticles followed a well used procedure with the goal of a final particle size of 20 nm. The results presented in Table 4.2 however suggests a particle diameter of approximately 12 nm. The process is very delicate, and the final size of the particles is mainly controlled by the concentration ratios of the metal salt and the reducing agent [33]. There is however also a strong dependence on both temperature and pH. Notes from the group also points out that the higher concentration of reducing agent used, the smaller the particles will get.

The concentrations used during this experiment were suited for synthesis at 90 °C. Boiling during the synthesis indicated higher temperatures of the solution, which might have led to evaporation of solvent and a change in concentrations. It is hard to say if one constituent evaporates faster than the other, but it will probably have an effect on the particle size. One more reason why a higher temperature might lead to smaller particles could be the increased diffusion and mechanical mixing. A larger amount of seed particles could be formed, which will mean less amount of gold available per seed.

The method of size determination of the particles, is also a known and well used method [32]. It is concluded to provide good estimations for the size of gold nanoparticles in the range of $5 - 100$ nm assuming monodispersity and geometrical accuracy. The monodispersity should be relatively high due to negatively charged citrate groups on the surfaces of the AuNPs, but this is not determined. The exact geometrical shape of the particles is not determined and would require other measurement techniques, for example electron microscopy.

5.1.2 3D Electrodes

The synthesis of the 3D-structured electrode as well as the reference measurements of bare gold electrodes versus 3D-structured electrodes show successful results. The calculations of active surface area and roughness factor match the values from work performed by Murata et al. [34] where a roughness factor of approximately 70 is reached after three AuNP castings. The

high roughness factor is the reason why the signal is approximately 10 times higher for 3D-structured electrodes than for bare gold electrodes in Figure 4.12.

A lower number of voltammetric cycles was used for the system than in the original protocol. The process of electrochemical cleaning, or in this case roughening of the surface, is performed under harsh conditions, and the affect of this on the MIP particles is not known. Therefore these precautions were taken even during the reference measurements. The reason for using the slightly bigger particles were because these were more similar in size with the MIP particles going to be used.

5.1.3 Polymer Immobilisation

The polymer immobilisation process turned out to not be as straight forward as was hoped for. The main idea was to create a dispersion of both polymer particles and AuNPs. This would be used instead of a pure AuNP dispersion for synthesis of the 3D-structured surface. The polymer particles would be incorporated in the created surface. The fact that the AuNPs were dispersed in water in which the polymers do not well disperse, was solved by dispersion in ethanol.

There are many unanswered question regarding this procedure. First of all, how the chemical cleaning affects the stability of the polymer particles. The pure presence of the polymer particles might also affect the stability of the surface structure resulting in ruptured structures and lower active area. Another problem might be residual acids in the MIP particles which will be addressed further on in this discussion.

The coverage of the electrode surface would also be an important parameter, will the immobilisation step give a similar amount of accessible MIP particles each time? If one wanted to analyse the prepared electrodes further, I would suggest using a SEM. With material sensitive surface scans it would be possible to differentiate the core-silica of the polymer particles from gold.

Another issue is that there might be a noticeable signal change from the MIP in this single molecule system. This does however not represent conditions in the human body. Hundreds of different molecules would interfere with the surface. Serotonin also has the unwanted property of creating large branched networks adsorbing to the electrode surface [18]. This would in principle mean that even if we incorporate MIP particles in the surface, we need to cover up the rest of the active surface area.

Therefore other immobilisation methods should also be considered. One

way could be to incorporate the MIP particles in different filtering layers. This approach has been used by many research groups ([7, 35, 36] et cetera), either by the means of imprinted electropolymerisation or by combination of electropolymerised layers containing MIP particles. There was unfortunately no time in this project for further analysis of polymer immobilisation on the electrodes.

5.1.4 CV Measurements

The results from measurements with the MIP and NIP prepared electrodes are not that revealing. A first look at the graphs in Figure 4.13 could suggest a successful immobilisation of MIP or NIP particles. The lower non-faradaic current than in Figure 4.12a means that the active surface area is smaller. This does however not equal to actual immobilisation. One obvious reason is the decrease in AuNP concentration during the preparation of the polymer particle and AuNP dispersion. The same total amount of liquid was used during the casting process which means that the total amount of AuNPs was lower. This could easily be verified by making sure the total amount of AuNPs is the same.

Further analysis of the graphs would also suggest that there after all is a difference between the MIP and the NIP electrode. This is true for these measurements, there was however no reproducibility of those results. There was also some disturbance present during the measurements exhibited by jumps in the data with no idea as to why.

As there were many uncertainties leading up to the measurements, it would be suggested to put more time into the immobilisation process before moving further into new measurements.

5.1.5 Electrochemistry Conclusion

As previously stated the electrochemical measurements were performed on not working MIP particles, which means that no good conclusions can really be drawn. The measurements did verify the oxidation peak of serotonin and that it is visible down to at at least 160 nM. A 3D-structured electrode surface can provide a much higher signal due to a larger active area. This would be a good implement to use in a future sensor where the maxium geometrical size might be limited.

A key factor is the actual immobilisation of the MIP particles of the electrode surface. This project used the approach of physical adsorption in

combination with the synthesis of 3D-structured electrodes. Not enough data was collected to neither deem it successful or unsuccessful.

5.2 Presynthesised Serotonin MIPs

5.2.1 Background

As previously stated the synthesis of Protocol 1 was based on previous work in the research group. It should be stated that that protocol had shown promising results earlier, but valuable information on analytical characterisation had gone lost during a relocation of the laboratory.

At the same time as Protocol 1 was synthesised, two other batches were prepared. The main difference between Protocol 1 and the others was the use of an ionic functional monomer instead of the acidic MAA. This is thought to produce a polymer better suitable for aqueous environments by reducing the importance of hydrogen bonding between monomer and template. The other two protocols were produced with MAA as functional monomers instead. They were also synthesised in different solvents.

5.2.2 Analytical Characterisation

One key piece of information that was not available from previous experiments was the rebinding solvent used and also by which means the analytical characterisation was performed. The first rebinding trials in this project were performed with RP-HPLC, where two different methods were found and applied [5, 28]. From the results (not shown) no conclusion could be made that the particles were functioning. Due to some uncertainties and the wish to perform faster rebinding tests equilibrium rebinding test was used instead.

Equilibrium rebinding tests were performed with fluorescence spectroscopy due to a much faster measurement time. When using FS the issue of choosing a suitable mobile phase for the characterisation process is also eliminated. FS is performed directly on the supernatant retrieved from the samples after centrifugation. Due to the autofluorescent properties of serotonin: with emission at 337 nm, and the fact that only this one compound was to analyse, the change was validated.

5.2.3 Presynthesised Serotonin MIPs Conclusion

Rebinding tests were performed on all the three polymers in different solvents without any promising results. The binding isotherms (not shown) showed no real difference between the MIP and the NIP particles. That the

particles did not work could also have been concluded from the fact that they did not display the pink color mentioned previously.

5.3 Serotonin Bulk Polymer

5.3.1 Protocol Selection

The next step of the project became to locate a reported working protocol of serotonin imprinting. Optimisation of a new protocol would have been a too time consuming task. There were two main problems with the choice of protocol: the amount of reports on successful serotonin imprinting are not too many, and the available reports are in many cases contradictive. A list was prepared mainly based on four articles where serotonin imprinting had been reported [5, 7, 19, 37]. The recipes were compared and the discussion and results of the different articles were tabled (not shown).

In all the cases EGDMA was used a cross-linker and MAA was used as a functional monomer. Some protocols also used a second uncharged functional monomer, either AM or MAam to neutralise the final polymer. In protocol [5] MAam is used and it is concluded that it shows a lot better result than only AM, whereas AM is the second functional monomer in protocol [7]. The porogen is widely varied between the protocols, it is either DMSO, DMF or toluene. Finally the choice of protocol landed on the newest report which also is the most cited one, [7]. In this article it was reported that the MIP showed good results in aqueous solution, highly relevant for the project.

5.3.2 Synthesis and Analysis

The MIP particles were synthesised as far as possible according to protocol, the procedure described in Section 4.2. In the beginning however, a different washing procedure was chosen. The reasons for this was the fact that the proposed Soxhlet extraction simply is a very time consuming process, one of its drawbacks [16]. It is also a process that is hard to monitor for quantitative analysis of template removal. The washing curves produced and shown in Figure 4.4 do however confirm, that even with another procedure and other chemicals, the template is removed from the MIP. Even though a different washing method was chosen, unfortunately no quantitative analysis of template removal was performed.

The binding isotherms shown in Figure 4.6 show no difference between MIP and NIP binding. They are also far away from the results in reference [7] which indicates a non-successful imprinting process. Results far away

from the theoretically calculated are not unusual and are due to effects of polymer treatments discussed in Section 2.3.

5.3.3 Troubleshooting

A great amount of troubleshooting was performed when it turned out that the MIP did not show any signs of imprinting. Common issues when it comes to polymer chemistry and molecular imprinting in general were addressed.

Functional Monomers

One part of the chosen protocol questioned, was the use of MAA and AM in combination. The two monomers are structurally more different than for example MAA and MAam which are used in [5], a paper in which AM was discarded as a functional monomer. Different structures will lead to different reactivity ratios of the radicals. This might lead to the synthesis of a copolymer instead of an even monomer composition throughout the polymer. The reactivity ratio product for both monomer pairs do however end up at similar values [38], around 2, which would not indicate any direct difference between the final polymer composition.

The template-monomer ratio is also an important factor during the synthesis. The functional monomer should usually be available at a concentration four times higher than that of the template. This is to get as high binding as possible. In the specific case of [7] the ratio of T:M was 1 : 2. This was slightly lower than reported in [5] and [19]. None of the protocols really discuss this and further measurements would be needed to explore the exact influences of this deviation. A simple approach would be the preparation of MIPs at these different ratios and then compare the results.

Serotonin Oxidation

As mentioned multiple times, serotonin is a molecule prone to oxidation and this was early on in the project considered one of the main reasons as to why the MIPs did not function. The oxidised structure of serotonin, as seen in Figure 2.5 would of course also be a possible imprinting template, but resulting affinity would probably be weaker, specifically for the non oxidised molecule. A very handy property of serotonin is the color change from off-white when non oxidised to a pinkish color in solution and a dark brown color of the synthesised polymer.

The authors of the chosen paper were contacted and some recommendations on preparation were received. To minimise oxidation they had prepared the polymerisation in amber coloured vials and in a cooled environment.

These tips were valued and used for batches MIP4-5, although some problems were encountered with the low temperatures, addressed later on in the discussion.

It seems counter-intuitive to use UV light as a source of initiation when this also might lead to oxidation of the sample. The authors of the article stated that this had low impact on the final MIP. Proton NMR measurements confirmed this, by showing non oxidised serotonin still in the sample after being exposed to the UV-light used. The hydrogen atoms of interest, numbers 8,7 and 13 in Appendix A and B are visible both before and after UV exposure.

Acid Residues

One other problem encountered during analysis of the bulk serotonin MIP was acid residues still inside the polymer. These are left behind from the template removal step and also need to be removed. Upon rebinding the acid residues would be freed in the solution and therefore be able to interact with the template. This would be a competitive binding with regard to the wanted binding between template and MAA inside the polymer. The result might mean low or no binding visible.

A simple pH measurement of the supernatant was utilised to visualise a very low pH for some of the polymers. If this was the case, a couple of extra steps of washing with water were performed. The pH would then be neutralised and stabilised. Unfortunately this would not result in any difference in rebinding for the MIPs.

The Porogen

DMSO is a polar aprotic solvent, its dielectric constant 47.24. Due to its polarity and structure, this solvent is more similar to water than other solvents often used for molecular imprinting which could mean a greater rebinding effect in aqueous conditions. Ref. [5] however concludes that DMSO influences the cavity formation too much, and therefore discard the use of this as a porogen. A higher imprinting effect was reached in DMF, a solvent with a lower dielectric constant. In [7] and [19] the highest imprinting factors are however shown for MIPs synthesised with DMSO as a porogen. Whereas Peeters et al. [7] does not discuss why this might be, Okutucu et al. [19] deals with this topic. It is stated that the poor hydrogen bonding properties of DMSO facilitates the hydrogen bond formation between template and AM monomers. The hydrogen bonded ion pairs that would

form between the basic template and the acidic monomers would however be hindered by the porogen polarity. The end result would be higher specific affinity.

One problem in working with DMSO is the very high freezing temperature at 18 °C. This resulted in some issues in working with cooled environments. The batches created in this project were smaller than the ones in the protocol facilitating freezing of the prepolymerisation mixture. Larger batches would however mean the use of more template than available, a template which is rather expensive. The two batches MIP4-5 were synthesised above the freezing temperature. Since this did not change the rebinding results this issue could be discarded.

A second problem with DMSO is its hygroscopicity; the ability to absorb water. This was finally suspected to have been one of the main reasons to non-functioning MIPs in this project. It is common for research groups to use the same porogen for different systems, if once proven functional. In this research group DMSO is rarely used and the bottle was unfortunately very old. Even though it was stored over molecular sieves it might have absorbed water from the air. Water in the system would not only disturb the polymerisation process, it would also be able to form hydrogen bonds both with the functional monomers and the template. If the DMSO was used to increase selectivity amongst the hydrogen bonds, but there was water in the system, this could be a reason as to why almost no sign of imprinting was visible in the synthesised polymers, even though all systems were purged well under nitrogen flow. This can however not be the only factor. Even polymers imprinted under non dry solutions, should show the same binding as the NIP particles. Not even this was the case.

5.3.4 Further Analysis of the Serotonin System

There are some further analysis methods which could be utilised to more accurately pin-point the exact reason as to why the serotonin MIPs were not working. First of all new batches using dry and new DMSO should be prepared. One should also prepare a couple of batches using different porogens for comparison purposes. When it comes to analysis of template-monomer interaction, NMR analysis is the most commonly used method. T:M ratios are easily determined by this, and exactly what type of bonds that are formed are also easier to monitor.

5.4 Histamine Bulk Polymer

The first histamine polymer that was synthesised (HMIP1) followed a protocol by the same research group behind the serotonin protocol. DMSO was once again used as a porogen but only one functional monomer was used (MAA). This polymer did also not show any sign of specific binding (results not shown). There was a quick decision to move to a different type of protocol using a different porogen.

The choice landed on a protocol by Trikka et al. [21]. Histamine imprinting protocols are more abundant and standardised which makes the selection process a bit easier. The protocol was used as an outline, and with knowledge from research group in Malmö, some of the constituents were exchanged. The functional monomer MAA, as well as the cross-linker EGDMA were kept. Both porogens used in the original protocol: chloroform and acetonitrile, were tried in batches HMIP3 and HMIP4. The initiator was however changed from AIBN to ABDV. It has a lower initiation temperature, but is therefore slightly harder to handle. The reason for the exchange was solely that this is a more common used initiator for the group in which the work was performed.

As stated, both porogens in the protocol were used for two synthesised batches. The result of both batches (comparison not shown) does not show a big difference. A quick analysis of MIP values minus NIP values however showed that the batch prepared in chloroform had slightly better properties, in agreement with the paper from Trikka et al. More analysis would be needed to confirm this, such as data fit to binding models and comparison of binding properties.

The binding isotherm in Figure 4.8 shows that the batch HMIP3 shows good selectivity for histamine in PBS solution. The data was fit to a non-linear binding model regarding MIP binding as the total bound analyte and NIP binding as non-specific binding. Usually data is fit to multiple models to see which one fits best. For this there were not enough data points in neither the linear region of the saturation region, and therefore a combination model was used. This means that the calculated values should not be fully trusted.

As the research group does a lot of work towards composite materials such as MIP core shell particles, the next step was to transfer this working MIP protocol to this format. There was only time for an initial batch which unfortunately did not show any promising result.

5.4.1 Cross-Reference Rebinding Test

The cross-reference rebinding shows that the synthesised histamine MIP particles that show good specific binding in pure histamine solutions, do unfortunately also show good binding to other similar structures such as serotonin. The serotonin binding is higher than that of histamine presumably explained by the hydrophobic nature of both serotonin and the EGDMA monomers in the polymer, it is however less specific: shown by the small binding differences between MIP and NIP. Both of the analytes are however washed away in a mixture of PBS and MeCN. This might not be too surprising since both hydrogen bonds and ionic interactions could be disrupted by the solvent constituents. Instead rebinding tests in a purely polar solvent such as MeCN or in a purely aqueous solvent could better confirm by which interaction type the analytes are bound. If it turns out that similar amounts of analytes are bound by hydrogen bonds, the synthesised MIP is successfully imprinted, it would just not be specific enough for the histamine sensor concept. Further cross-reference rebinding tests should also be performed regarding other interfering molecules.

5.5 Future Prospects

The project did for a couple of reasons take longer time than planned which did lead to some roads unexplored. Already at the time at which the first results for HMIP3 was reached, not much time was left which limited the amounts of tries possible to determine for example template removal during washing. So if the project was to continue, adequate MIP analysis would be the first checkpoint. It would then make sense to prepare a new serotonin MIP batch with new DMSO, and try to get closer to the solution as to why this imprinting protocol was not reproducible. Further investigation of the core-shell approach would also be interesting work.

Regarding the electrochemical measurements there are also experiments that would bring reason to some of the unanswered questions. SEM measurements of the immobilisation might be one option. One could also try the physical adsorption on the already 3D-structured surface. If working with the RAFT polymerised particles it would be possible to utilise thiol chemistry to chemically bind the MIP particles to the gold surface. It would however only make sense to continue the electrochemistry once a sufficiently MIP has been extensively analysed.

6

Conclusion

This project has dealt with the field of MIP technology. The aim was to synthesise and analyse MIP particles showing a high affinity to the neurotransmitters serotonin and histamine for the potential use in an amperometric sensor. These would then be incorporated into a device that could be able to detect physiologically relevant concentrations of the analytes from relevant liquids. A lot of trouble was met during the course of the work performed and this led to lowering of the aims and a focusing on the MIP systems.

The initial testing of a prepolymerised serotonin MIP did not provide any results, mainly because the particles were not functioning but even so the methods used for electrochemical testing still has to go through some optimisation before further experiments. A protocol of serotonin imprinting reported to work well was unsuccessfully reproduced, even after intense troubleshooting. Instead histamine MIPs were synthesised combining a reported protocol together with the knowledge of the responsible supervisors. These particles showed specific rebinding properties in rebinding histamine from a single molecule system but also showed high binding concentrations for serotonin. Limited by time, some of the typical analysis experiments were not completely finished, such as the quantitative analysis of template removal.

Unfortunately there was also not enough time left of the project to perform any new electrochemical measurements on the working histamine MIP. Based on the fact that the histamine MIP particles do not show any promising results in a multiple molecule system this might on one hand have been good. On the other hand, the immobilisation techniques could easily be validated in a single molecule system, and seeing that this is a crucial part of the sensor application the experiment would still have made sense.

The project as such might not have rendered any scientifically relevant results, but the aims were from the beginning high, and the time working

on the project has given me a deeper knowledge in many more fields than I from the beginning could have anticipated. This project could easily have been continued another couple of months or even years. The work of MIP optimisation and revelation of new MIP recipes is still a place where a lot of work needs to be done.

References

(1) Haupt, K.; Mosbach, K. *Chemical Reviews* **2000**, *100*, 2495–2504, DOI: 10.1021/cr990099w.

(2) *Serotonin Receptor Technologies*, 1st ed.; Blenau, W., Baumann, A., Eds.; Humana Press: 2015, DOI: 10.1007/978-1-4939-2187-4.

(3) King, M. W. Brief overview of the Human Nervous system., 2015, http://themedicalbiochemistrypage.org/nerves.html#5ht.

(4) Lee, G. S.; Simpsons, C.; Sun, B. H; Yao, C.; Foer, D.; Sullivan, B.; Matthes, S.; Alenina, N.; Belsky, J.; Bader, M.; Insogna, K. L. *Journal of Bone and Mineral Research* **2014**, *29*, 976–981, DOI: 10.1002/jbmr.2086.

(5) Khurshid, S. S.; Schmidt, C. E.; Peppas, N. A. *Journal of Biomaterials Science* **2011**, *22*, 343–362, DOI: 10.1163/092050610X486955.

(6) Picca, R. A.; Malitesta, C.; Mohammadi, R.; Ghorbani, F.; Sellergren, B. In, Baldini, F., D'Amico, A., Di Natale, C., Siciliano, P., Seeber, R., De Stefano, L., Bizzarri, R., Andó, B., Eds.; Sensors, Vol. 162; Springer: New York, 2014, pp 165–169, DOI: 10.1007/978-1-4614-3860-1_29.

(7) Peeters, M.; Troost, E. J.; van Grinsven, B.; Horemans, F.; Alenus, J.; Murib, M. S.; Keszthelyi, D.; Ethirajan, A.; Thoelen, R.; Cleij, T. J.; Wagner, P. *Sensors and Actuators B: Chemical* **2012**, *171-172*, 602–610, DOI: 10.1016/j.snb.2012.05.040.

(8) Andorolov, V.; Shleev, S.; Thomas, A.; Ruzgas, T. *Analytical and Bioanalytical Chemistry* **2013**, *405*, 3871–3879, DOI: 10.1007/s00216-013-6756-x.

(9) Yan, M.; Ramström, O., *Molecularly Imprinted Materials: Science and Technology*; Marcel Dekker: New York, 2004.

(10) Sellergren, B.; Hall, A. J. In, Steed, J. W., Gale, P. A., Eds.; Supramolecular Chemistry: From Molecules to Nanomaterials; John Wiley & Sons, Ltd.: 2012, pp 3255–3282, DOI: 10.1002/9780470661345.smc137.

(11) Sellergren, B. In; Molecularly Imprinted Polymers: Man-Made Mimics of Antibodies and their Application in Analytical Chemistry; Elsevier: Amsterdam, 2001, pp 113–184, DOI: 10.1016/S0167-9244(01)80008-1.

(12) Ye, L.; Mosbach, K. *Journal of Inclusion Phenomena and Macrocyclic Chemistry* **2001**, *41*, 107–113, DOI: 10.1023/A:1014498404292.

(13) *Molecular Imprinting: Principles and Applications of Micro- and Nanostructured Polymers*; Ye, L., Ed.; Pan Stanford Publishing Pte. Ltd.: Singapore, 2013.

(14) Cowie, J. M. G.; Arrighi, V., *Polymers: Chemistry and Physics of Modern Materials*, 3rd; CRC Press: Boca Raton, 2008.

(15) Mohammadi, R. Molecularly Imprinted Core-Shell Nanoparticles by Surface Initiated RAFT Polymerization., Ph.D. Thesis, 2014.

(16) Lorenzo, R. A.; Carro, A. M.; Alvarez-Lorenzo, C.; Concheiro, A. *International Journal of Molecular Sciences* **2011**, *12*, 4327–4347, DOI: 10.3390/ijms12074327.

(17) Chattopadhyay, A.; Rukmini, R.; Mukherjee, S. *Biophysical Journal* **1996**, *71*, 1952–1960, DOI: 10.1016/S0006-3495(96)79393-1.

(18) Patel, A. N.; Unwin, P. R.; Macpherson, J. V. *Physical Chemistry Chemical Physics* **2013**, *15*, 18085–18092, DOI: 10.1039/C3CP53513D.

(19) Okutucu, B.; Telefoncu, A. *Talanta* **2008**, *76*, 1153–1158, DOI: 10.1016/j.talanta.2008.05.033.

(20) Lange, J.; Wittmann, C. *Analytical and Bioanalytical Chemistry* **2002**, *372*, 276–283, DOI: 10.1007/s00216-001-1130-9.

(21) Trikka, F. A.; Yoshimatsu, K.; Ye, L.; Kyriakidis, D. A. *Amino Acids* **2012**, *43*, 2113–2124, DOI: 10.1007/s00726-012-1297-8.

(22) Horemans, F.; Alenus, J.; Bongaers, A.; Weustenraed, R.; Thoelen, R.; Duchateau, J.; Lutsen, L.; Vanderzande, D.; Wagner, P.; Cleij, T. J. *Sensors and Actuators B: Chemical* **2010**, *148*, 392–398, DOI: 10.1016/j.snb.2010.05.003.

(23) Harvey, D. In, Electronic Version; Analytical Chemistry 2.0, 2008, pp 667–782, http://www.asdlib.org/onlineArticles/ecourseware/Text_Files_files/Chapter11.pdf.

(24) *Biosensors Fundamentals and Applications*; Turner, A. P. F., Karube, I., Wilson, G. S., Eds.; Oxford University Press: New York, 1987.

(25) Carvalhal, R. F.; Freire, R. S.; Kubota, L. T. *Alectroanalysis* **2005**, *17*, 1251–1259, DOI: 10.1002/elan.200403224.

(26) Andoralov, V.; Falk, M.; Suyatin, D. B.; Granmo, M.; Sotres, J.; Ludwig, R.; Popov, V. O.; Schouenborg, J.; Blum, Z.; Shleev, S. *Scientific Reports* **2013**, *3*, DOI: 10.1038/srep03270.

(27) Sigma-Aldrich Solvent Center., 2015, http://www.sigmaaldrich.com/chemistry/solvents/products.html.

(28) Xiao, R.; Beck, O.; Hjemdahl, P. *Scandinavian Journal of Clinical and Laboratory Investigation* **1998**, *58*, 505–510, DOI: 10.1080/00365519850186319.

(29) Lemaire, P. A.; Adosraku, R. K. *Phytochemical Analysis* **2002**, *13*, 333–337, DOI: 10.1002/pca.659.

(30) Quickenden, T. I.; Irvin, J. A. *The Journal of Chemical Physics* **1980**, *72*, 4416–4428, DOI: 10.1063/1.439733.

(31) Grabar, K. C.; Freeman, R. G.; Hommer, M. B.; Natan, M. J. *Analytical Chemistry* **1995**, *67*, 735–743, DOI: 10.1021/ac00100a008.

(32) Haiss, W.; Nguyen, T. K. T.; Aveyard, J.; Fernig, D. G. *Analytical Chemistry* **2007**, *79*, 4215–4221, DOI: 10.1021/ac0702084.

(33) Kimling, J.; Maier, M.; Okenve, B.; Kotaidis, V.; Ballot, H.; Plech, A. *Journal of Physical Chemistry B* **2006**, *110*, 15700–15707, DOI: 10.1021/jp061667w.

(34) Murata, K.; Kajiya, K.; Nukaga, M.; Suga, Y.; Watanabe, T.; Nakamura, N.; Ohno, H. *Electroanalysis* **2010**, *22*, 185–190, DOI: 10.1002/elan.200900323.

(35) Li, Y.; Liu, Y.; Liu, J.; Liu, J.; Tang, H.; Cao, C.; Zhao, D.; Ding, Y. *Scientific Reports* **2015**, *5*, 1–8, DOI: 10.1038/srep07699.

(36) Mazzotta, E.; Picca, R. A.; Malitesta, C.; Piletsky, S. A.; Piletska, E. V. *Biosensors and Bioelectronics* **2008**, *23*, 1152–1156, DOI: 10.1016/j.bios.2007.09.020.

(37) Kitade, T.; Kitamura, K.; Konishi, T.; Takegami, S.; Okuno, T.; Ishikawa, M.; Wakabayashi, M.; Nishikawa, K.; Muramatsu, Y. *Analytical Chemistry* **2004**, *76*, 6802–6807, DOI: 10.1021/ac040098q.

(38) *Polymer Handbook*, 3rd; Brandrup, J., Immergut, E. H., Eds.; John Wiley & Sons: 1989.

Appendicies

Appendix A

NMR spectrum of serotonin in deuterated DMSO.

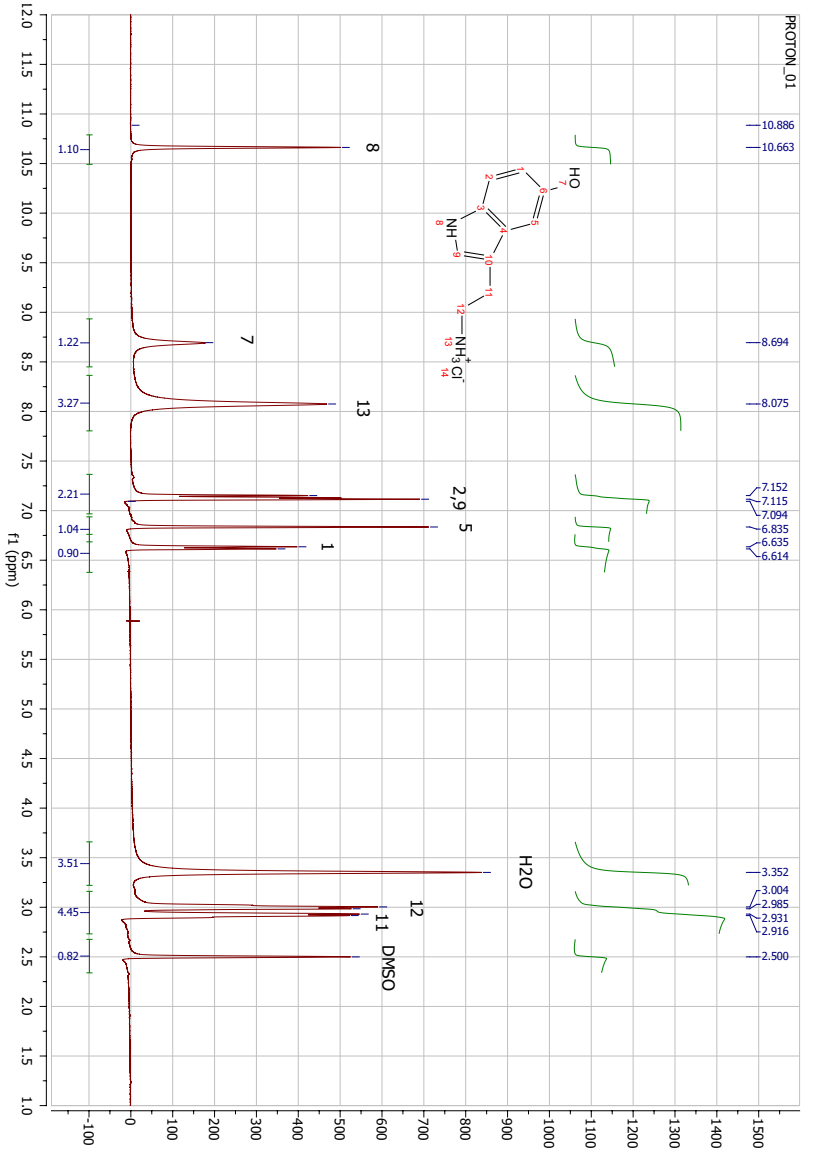

Appendix B

NMR spectrum of serotonin in deuterated DMSO subjected to UV-light.